2016

Corn stover biochar in gypsum board: Empirical analysis of thermal conductivity and flexural strength

Albena Yordanova
University of Northern Iowa

CORN STOVER BIOCHAR IN GYPSUM BOARD: EMPIRICAL ANALYSIS OF THERMAL CONDUCTIVITY AND FLEXURAL STRENGTH

An Abstract of a Dissertation
Submitted
in Partial Fulfillment
of the Requirement for the Degree
Doctor of Technology

Approved:

_____
Dr. Lisa Riedle, Committee Chair

_____
Dr. Kavita Dhanwada
Dean of the Graduate College

Albena Yordanova

University of Northern Iowa

December 2016

ABSTRACT

Gypsum board, an economical and durable finish material for wall and ceiling construction in the United States and worldwide, is the component with the lowest thermal performance in a typical exterior wall assembly. It also constitutes a substantial portion of construction waste in landfills, potentially creating harmful environmental effects and dangerous gases. To minimize the negative effects of fast growing construction waste of gypsum in landfills and meet higher standards for energy efficiency in construction, there is a need to explore sustainable ways of improving thermal properties of gypsum board and recycling the material. Gypsum can be recycled and used in agriculture as an agent for soil amendment and means of water retention.

Climate change and global warming lead to water scarcity. It is necessary to consider potential soil amendments that could improve the environment. Biochar, known to ancient Amazon Valley cultures as long-term soil amendment, is currently becoming abundantly available as a waste product of bio fuel production.

Biochar and gypsum were used in the present study to improve the performance of gypsum board by studying the thermal conductivity, density, and flexural strength of a biochar-gypsum composite. The findings of this research proved that inclusion of biochar in gypsum decreased the thermal conductivity, flexural strength, and density of the composite. The results from the flexural strength test indicated that including biochar within certain range produced a composite meeting, and in some case exceeding, the current ASTM C 1396 standard.

The results of this study can be used as a basis for future research, potentially creating a bio-based composite material for finishing walls and ceiling, fully recyclable into soil amendment, and acting as a factor for carbon sequestration.

CORN STOVER BIOCHAR IN GYPSUM BOARD: EMPIRICAL ANALYSIS OF THERMAL CONDUCTIVITY AND FLEXURAL STRENGTH

A Dissertation

Submitted

in Partial Fulfillment

of the Requirement for the Degree

Doctor of Technology

Approved:

_____

Dr. Lisa Riedle, Chair

_____

Dr. Nilmani Pramanik, Co-Chair

_____

Dr. Hong (Jeffrey) Nie, Committee Member

_____

Dr. Robert Boody, Committee Member

_____

Dr. Kimberly MacLin, Committee Member

Albena Yordanova

University of Northern Iowa

December 2016

DEDICATION

To my mother Pavlina, my father Yulian, my brother Hristo for loving me and being there for me all my life, to my nouno Spiro and my nouna Yiota, Mary and Bill Keys, and all my Bulgarian, American, Australian, and Greek friends, for believing in me, and to Sophie and Honey for listening, and understanding.

To my amazing daughter Pavleena, I love you more than the entire world!

ACKNOWLEDGEMENTS

Over the past eight years I have received support and encouragement from a great number of individuals. I would like to express my special appreciation and thanks to my major advisor Dr. Lisa Riedle, without whose support this research could not have been completed. I would like to thank you for encouraging my research and your guidance. I would like to thank my dissertation committee members, Dr. Nilmani Pramanik, Dr. Hong (Jeffrey) Nie, Dr. Robert Boody, and Dr. Kimberly MacLin for their support over the years as I moved from an idea to a completed study. I also thank Dr. Junyong Ahn for his valuable advice, Dr. John T. Fecik, and Dr. Shahram VarzaVand for their support during my studies. During data collection and writing Byron G. Garry spent countless hours helping me with the experimental setup and proofreading. Byron's support, ideas, and technical knowledge made the project a success. Special thanks to Byron T. Scott who generously offered me editing help when I most needed it. My deepest gratitude to Dr. Teresa K. Hall, Dr. ZhengRong Gu, and Dr. Erin Cortus who provided so much needed encouragement and helped me with their expertise. I have learned much though our conversations. Finally, thanks to Mary Keys, Bryce Cooper, Stoyanka Pashova, Vassilka Stoycheva, DeAnn Parsons, and Anelia Dimitrova for giving me a push to keep working to the completion of this research study.

TABLE OF CONTENTS

LIST OF TABLES

TABLE PAGE

LIST OF FIGURES

FIGURE PAGE

CHAPTER 1

INTRODUCTION

Statement of the Problem

The problem that this research sought to solve was addressing the lack of experimental research on the inclusion of biochar on thermal and strength performance of gypsum board. As in most other fields, the architecture, engineering and construction (AEC) professionals are faced with increasing demands for sustainability. Increasing energy efficiency, reducing waste, and using recyclable materials, are the heart of sustainability considerations in construction and operations of buildings. Performance-based standards require higher demands on design of an energy-efficient building envelope, the components separating conditioned from non-conditioned space in buildings (ASHRAE, 2015). The progressively more stringent standards on sustainable and energy-efficient building envelopes require optimization of all materials in the building envelope. Durability, improved thermal performance, and adaptability for reuse or recycle are the most critical properties of new and traditional building materials.

Statement of Purpose

The purpose of this experimental study was to explore the effects of corn stover biochar on thermal resistance, density, and flexural strength of gypsum board. In this research flexural strength was used as a proxy for durability, as the latter cannot be tested by ASTM standards. This study was unique in that it explored these adverse properties of the composite bio-based material to provide a base for practical application in construction.

The results of this study could be used to create an improved bio-based composite material which will benefit both the inhabitants of the buildings and the environment.

Statement of Need

The need and justification of this study were based on the lack of empirical studies on the effect of biochar's inclusion in gypsum materials. The review of the literature indicated extensive empirical research during the past couple of decades on improving thermal properties in building materials in general, and in gypsum board specifically, by the inclusion of phase change materials (Feldman, Banu, Hawes, & Ghanbari, 1991; Feustel & Stetiu, 1997; Kosny, Shukla, & Fallahi, 2013; Schossig, Henning, Gswander, & Haussmann, 2005). Research has also been done using the inclusion of rubber from automobile tires in gypsum to improve the thermal performance of gypsum board (Abu-Lebdeh, Fini, & Fadiel, 2014). However, the literature review found no empirical studies of the effect of adding biochar on thermal and physical properties of gypsum board.

Background

The Department of Energy (DOE) defined building envelope as all components of a building, or a structure, which separate conditioned space from non-conditioned space (US Department of Energy, 2015). They also defined building materials as any element, excluding air films or insulation, of the building envelope, that is included in the calculations of the component's thermal insulation (US Department of Energy, 2015).

Gypsum board is the building material with lowest thermal insulation value (R-value) after that of poured concrete (ColoradoENERGY, 2013). Gypsum board has an R-value from 0.33 for 3/8” board to 0.83 for 1” board (Gypsum Association, 2010).

The latest version of Leadership in Energy and Environmental Design (LEED) v4, the universally accepted rating system for sustainability rating of buildings, recommends choosing bio-based materials, as bio-based materials most often have fewer harmful effects on the environment and meet Sustainable Materials and Resources (MR) credits for multi-attribute optimization (McCombs, 2015). The intent of this rating system is to encourage use of environmentally preferable materials and products. The stress is on preference of sustainable characteristics and reusable products with bio-based content over traditionally used disposable and unhealthy materials and products.

Researchers focus on improving sustainability by using wastes of production processes to create new building materials. Converting waste from one production into resources for another promotes economic growth in developing industries and environmental sustainability. Closed-loop material management requires that a by-product from one source becomes a resource for another (Garcia-Perez, Lewis, & Kruger, 2010). Enhancing the thermal properties of gypsum board by even a small increment would improve the energy performance of the building envelope manifold.

By decreasing the thermal conductivity of gypsum board, the total R-value of the exterior walls would improve. Recent studies focused on improving the thermal resistance of gypsum board by adding waste rubber (Abu-Lebdeh et al., 2014), or lightweight additives such as perlite and vermiculate (Allen & Iano, 2014 & Simmons,

2011), or polyurethane wastes to gypsum (Gutiérrez-González, Gadea, Rodríguez, Junco, & Calderón, 2011).

Gypsum Board

Today, gypsum in the form of gypsum wall boards (GWB) is used as finish material on more that 90% of interior walls and ceilings in the United States, making it one on the most popular materials used in construction worldwide (US Geological Survey, 2014). Fire resistance, sound attenuation, durability, economy, and versatility are the properties that make it the preferred choice of finish building material for interior applications as well as part of the building envelope (Simmons, 2011; Kibert, 2013).

Biochar

The term biochar is used today to refer to the solid material produced from biomass of wood or leafy plant materials in an environment with very low or no oxygen levels at all. Biochar is the solid by-product of biofuel production from biomass in an oxygen-deprived environment (Peláez-Samaniego, Garcia-Perez, Cortez, Rosillo-Calle, & Mesa, 2008). Production of biochar is still largest in countries where it has been used for agricultural applications. With the growing interest in bio-energy sources, biochar production is increasing in more technologically developed countries. In 2005, the world production of biochar was more than forty four million tons. Biochar currently yields about 20% of the weight of the original biomass (Garcia-Perez et al., 2010).

Additionally, reducing the amount of natural gypsum mined for the construction industry, by replacing a portion with biochar, would have a positive effect on the environment and would preserve this non-renewable resource for future generations.

Statement of Hypotheses

This research sought to determine the range of biochar inclusion for optimized biochar-gypsum mix with better thermal insulation value and comparable standard flexural strength. For that reason the researcher stated the following hypotheses:

$H_0$1: There is no difference between the thermal conductivity of biochar-gypsum mix and the thermal conductivity of gypsum alone.

Ha1: There is a statistically significant difference between the thermal conductivity of biochar-gypsum mix and the thermal conductivity of gypsum alone.

$H_0$2: There is no difference between the flexural strength of biochar-gypsum mix and the flexural strength of gypsum alone.

Ha2: There is a statistically significant difference between the flexural strength of biochar-gypsum mix and the flexural strength of gypsum alone

$H_0$3: There is no difference between the density of biochar-gypsum mix and the density of gypsum alone.

Ha3: There is a statistically significant difference between the density of biochar-gypsum mix and the density of gypsum alone.

The researcher expected that with the increase of biochar content, the thermal conductivity and density of the composite would decrease. The researcher also expected that an adverse effect, lower flexural strength of the composite, would be within a range suitable for practical applications.

The results of this study can be beneficial to the building industry as new bio-based material with improved thermal performance as well as minimizing the waste of gypsum in landfills.

Assumptions

The following assumptions were made in pursuit of this study:

1. Tap water from a single source did not vary significantly in properties and did not affect the properties of the control and experimental groups.
2. Gypsum (Plaster of Paris) used in this study did not vary significantly in properties.
3. The hot box apparatus and test procedure produced statistically valid data.

Limitations

The following limitations were noted:

1. The study was limited to determining only three physical properties of biochar-gypsum mix. To determine durability of the product more properties need to be tested under various service conditions over a substantial period of time.
2. The range of temperature for running the thermal conductivity test was limited to the maximum temperature rating of the HFP01 heat flux sensor used.
3. The results from the flexural strength test and the thermal conductivity test can not be compared to those of manufactured gypsum products due to difference in mixing and casting processes.

Delimitations

The following limitations were made by the researcher due to time constraints:

1. Only corn stover biochar was studied, other types of biochar were beyond the scope of the study.
2. One range size corn stover biochar was used. Other sizes of biochar were beyond the scope of this study.
3. Commercially available white plaster of Paris was used. The varying formulations of plaster of Paris were beyond the scope of this study.
4. Only tap water from Brookings, South Dakota, was used for the study.
5. Five different design mixes of different ratios of corn stover biochar (10, 20, 30, 40, and 50%) were used.
6. Only five specimens of each design mix of biochar-gypsum mix were made and five control specimens of standard plaster of Paris.
7. All test specimens were 12”x 12” x ½” in size.

Definitions of Terms

The following terms were defined to clarify their use in the context of the study:

Gypsum: “An abundant mineral in nature, a crystalline hydrous calcium sulfate” (Allen & Iano, 2014, p. 893).

Gypsum board: "…the generic name for a family of sheet products consisting of a noncombustible core primarily of gypsum, with paper surfacing." (ASTM International, 2014b, p. 3).

Biomass: "…the product of photosynthesis from carbon dioxide and water" (Lee et al., 2013, p. 196).

Biochar: "...pyrolysis of biomass produces three products: one liquid, bio-oil, one solid, bio-char and one gaseous (syngas)" (US Department of Agriculture, 2014, p.1).

Flexural strength is defined as the ability of a material to "resist deformation under load" (MatWeb, 2015, p. 1).

Thermal conductivity: "The rate of heat flow, under steady conditions, through unit area, per unit temperature gradient in the direction perpendicular to the area. It is given in the SI units as Watts per (meter - Kelvin)" (The Engineering Toolbox, n.d., p. 1).

Appendix A contains a list of definitions of other terms used in this study for understanding their use in the context of this research.

CHAPTER 2

REVIEW OF THE LITERATURE

This research focused on improving the thermal performance of gypsum products by the inclusion of corn stover biochar, and the effect of biochar on flexural strength of the composite. A review of the traditional practices was included in this chapter to provide background information and context for the new trends in AEC industries in general, and building envelope improvement in particular.

There were two groups of topics that were explored in the literature review section of this study. The first group focused on trends as applied to AEC practices. These included (a) governmental and public initiatives promoting sustainability in buildings, and (b) the consistently more stringent energy and building codes. The second group focused on the properties, and application of gypsum board and biochar.

Initiatives

The U.S. Environmental Protection Agency (EPA) recognizes the construction and operating of buildings involves enormous amounts of energy, water, and other resources, as noted by Allen and Iano (2014) “In the United States, buildings consume approximately 35 percent of this country’s energy, 65 percent of its electricity, 12 percent of its potable water, and 30 percent of its row materials” (p. 5). Further, they create substantial amounts of waste. At the same time, the construction industry has a significant impact on the environment and indoor air quality for inhabitants. The literature indicates that the building sector consumes more than 40% of the total energy in the European Union (Drochytka, Zach, Korjenic, & Hroudove, 2013). As demands on

reducing buildings energy consumption become more stringent, the manufacturers need to adapt their products to new regulations. In addition, resource exhaustion and waste production and disposal are becoming issues for governments worldwide.

Fast-growing energy consumption in the past decades created a need for energy efficient buildings worldwide. According to the United States Green Build Council (USGBC Research Committee, 2008), commercial and residential buildings are responsible for 38% of carbon dioxide emissions and 40% of non-industrial waste. Further, 39% the total energy used by US residential and commercial buildings was due to heating, ventilation, and air-conditioning (HVAC), 14% was due to lighting, and the remaining 47% was other uses. Hence, building Research and Development (R&D) in the construction industry must focus on creating and implementing energy efficient building envelope systems. A successful solution to the growing energy consumption and environmental concerns is closed–loop material management in which waste materials from one production can be used as feedstock, for a different production or recycled back into the original one.

The ASHRAE, USGBC, and the General Services Administration (GSA) have established high performance design standards for new buildings, focused on energy–efficient building envelope, and use of recovered, bio-based, energy-efficient, materials (GSA, 2015). Table 1 shows that gypsum board is listed as one of the five key sustainable products:

Table 1

Five Key Sustainable Products

Product	Sustainability Standard
Nylon carpet	NSF 140 Gold Certification *and* ≥ 10% post-consumer recovered content
Interior Latex Paint	≤ 50 grams/Liter (g/L) VOCs post-tint (SCAQMD Rule 113 standard)
Gypsum Board	Greenguard Gold certification
Acoustical ceiling tiles	Meets the California Section 01350 standard for low VOC materials Total recycled content ≥ 20% *and* Recyclable in a closed loop process *and* USDA Certified BioPreferred *and* Environmental Product Declaration (EPD) available
Concrete (ready-mix and site-mix)	≥15% fly ash or ≥ 25% ground granulated blast-furnace (GGBF) slag

Source: GSA, 2015

The Department of Energy (DOE) is conducting ongoing research, together with the National Association of the Home Builders, seeking to develop a wall system with R-20, R-30, and R-40 ratings. The research seeks to improve past wall system performance (Kochkin, 2010).

The Building Technologies Office (BTO) collaborates with the commercial building industry to improve energy efficiency of new and existing commercial buildings striving to reduce energy consumption across the commercial sector by at least 1,600 TBtu (Office of Energy Efficiency, 2014b). BTO also works with the residential building industry to improve energy efficiency of new and existing homes; BTO aims at reducing

energy consumption across the residential sector by a minimum 50% through developing and deploying cost–effective solutions. (Office of Energy Efficiency, 2014b).

The Building Envelope

The building envelope is "the interface between the interior of the building and the outdoor environment, including the walls, roof, and foundation" (Pew Center on Global Climate Change, 2011, p. 1). The building envelope plays a significant function in energy consumptions and comfort for the inhabitants. Acting as the thermal barrier between the outside and the interior, the building envelope plays a crucial role for reducing energy use and the resulting effect on the environment. Governmental weatherization programs, therefore, focus on improvement of the building envelope as the most effective way to save energy.

Improvement of the building envelope can be done in two basic ways: by overall design and by materials and product selection. Criteria for building envelope materials and product selection include increased thermal insulation.

Sustainability standards for materials selection are based on embodied energy, referring to the energy required to extract, manufacture, transport, install and dispose of building material. Efforts to reduce embodied energy use and the related harmful emissions include substitution by bio-based products.

The R Value of ½ inch gypsum board is 0.45 R/Inch hr·ft^2·°F/Btu and 5/8" 0.56 R/Inch hr·ft^2·°F /Btu (ColoradoENERGY, 2013). A comparative estimate of the R-value for exterior wall is given in Table 2:

Table 2

Component R Values in a Building Envelope

Component	R-value
Wall - Outside Air Film	0.17
Siding-Wood Bevel	0.80
Plywood Sheathing - 1/2"	0.63
3 1/2" Fiberglass Batt	11.00
1/2" Drywall	0.45
Inside Air Film	0.68
Total Wall Assembly R-Value	13.73

Source: ColoradoENERGY, 2013

Also ColoradoENERGY (2013) listed the R-values in the same range as gypsum board for concrete block 4” -0.80, poured concrete-0.08, and hardboard-0.34. R-value of an assembly is calculated as a sum of R-values of all components. Thus, it can be seen that the gypsum board is typically the component with the lowest or next to the lowest R-value in a wall assembly, and therefore any improvement in R-value of the gypsum board would increase the overall R-value of the entire assembly.

Abu-Lebdeh et al. (2014) conducted a study of the thermal conductivity of rubberized gypsum board in an effort to explore alternative use of recycled rubber from the automotive industry to improve the thermal resistance of gypsum board. Their study concluded that adding scrap rubber decreased thermal conductivity of gypsum board. Gutiérrez-González et al. (2011) found that adding polyurethane foam wastes to gypsum plaster also decreased thermal conductivity of the composite material.

Neither of the past studies aiming at improving the thermal performance of gypsum board conducted flexural strength tests. As strength of gypsum board is critical

for building purposes, the researcher tested both thermal conductivity and flexural strength of the composite product.

Gypsum and Gypsum Board

Gypsum, a mineral found in nature abundantly, is chemically crystalline hydrous calcium sulfate. It is quarried, or mined, crushed, dried, and ground to a fine powder, and finally heated to 350 degrees Fahrenheit (175^0C). The process is known as calcining, in which about three quarters of the water of hydration is eliminated. The calcined gypsum is then ground to a fine powder, mostly known as plaster of Paris. When mixed with water, plaster of Paris rehydrates and recrystallizes fast back to solid state. In the process, it releases heat and expands insignificantly (Allen & Iano, 2014).

Gypsum is a major component of interior finish material in the majority of buildings. It is comparatively durable, lightweight, and has good sound insulation capacities. It is also inexpensive, highly moldable, and resists the passage of fire. By increasing the thickness of the gypsum, virtually any requirement for fire resistance can be achieved. An alternative way to increase the fire ratings of gypsum is adding lightweight aggregates to reduce its thermal conductivity and by adding reinforcing fibers to retain the calcined gypsum in place as fire barrier (Simmons, 2011).

For use in construction, calcined gypsum is formulated with different admixtures to control setting time and other characteristics. For centuries, calcined gypsum was used for the production of gypsum plaster. When mixed with water, sand, and lightweight aggregates, such as perlite or vermiculate, calcined gypsum forms gypsum plaster were

used for interior applications. Gypsum plasters are manufactured today in accordance with ASTM C 28 (ASTM International, 2014c).

Gypsum board is made from gypsum plaster sandwiched between paper coverings. The most common ingredients in gypsum board are calcined gypsum, water, and paper. Gypsum board can also be produced in a range of thicknesses. For exterior and interior applications, where substantial levels of moisture are present, portland cement-lime plaster, known also as stucco, is commonly used in wall assemblies.

Gypsum board, a prefabricated plaster sheet manufactured in widths of 4 feet and lengths of 8 to 14 feet, is the least expensive of all interior finish materials for walls and ceilings (Simmons, 2011).The core of the gypsum board is formulated as a slurry of calcined gypsum, starch, water, and additives, and then the slurry is sandwiched between two layers of paper and pressed by a set of rollers to reach the desired thickness. In a couple of minutes, the material has hardened and bonded to the paper and is ready to be cut to length and heated to drive off residual moisture, then bundled for shipping.

There are several types of gypsum board produced to fit various applications: regular gypsum board, Type X gypsum board for fire-rated assemblies, in which short glass fiber is added to hold the calcined gypsum in place, Type C gypsum board which is more fire resistant, water-resistant gypsum backing board with moisture–resistant core formulation, and water-repellant paper of glass matt facings (Simmons, 2011).

Most gypsum board products are manufactured in accordance with ASTM standard C1396; gypsum board thicknesses vary from ¼ inch to 1 inch (ASTM International, 2014g).

Flexural Strength of Gypsum Board

While a crucial attribute of most building materials and components, durability is difficult to predict. Durability of a product is determined by the combination of: innate physical properties, the environment, design, installation, of the building material or component, and involves years of service before failure (ASTM Committee E-6, 1999). Gypsum board is manufactured to comply with ASTM C1396 which defines the minimum performance criteria for specific physical properties.

Addition of biochar to gypsum is expected to reduce the density of the mixture and consequently result in a decrease in flexural strength. As a rule decreased density of a material is related to decreased thermal resistance, but also to lower strength and durability in the long run. ASTM Symposium on durability of building materials defines durability as follows: “Durability-the capability of maintaining the serviceability of a product, component, assembly, or construction over a specified time” (Frohnsdorff & Masters, 1980, p. 18).

While prediction of durability of building materials and components is complicated and prone to errors due to unpredictable changes in environment over the service life, ASTM has no established test for durability, but defines procedures for testing the physical properties of building materials and components. When asked about tests for durability of gypsum board, Robert Wessel, FASTM, Senior Director, Technical Services, Gypsum Association (Wessel, personal communication, April 10, 2015) wrote: “Gypsum board is manufactured to comply with ASTM C1396 which defines the

minimum performance criteria for specific physical properties. The physical test methods used are described in ASTM C473."

For the purpose of this research the test for flexural strength as defined by ASTM C473 Method A (ASTM International, 2014e) for flexural strength was conducted to test the physical properties of biochar gypsum mix.

Biochar

The use of industrial waste to produce sustainable building materials has been a hot topic in research recently. Substitutions of materials with hazardous environmental effects are becoming the norm in research and design (R&D) in building materials. Fly ash substitutes are added to in concrete production to reduce the needs of cement production (Allen & Iano, 2014; Simmons, 2011). Production of biofuels, which use biomass, a waste of agriculture, constitute substantial sector of the energy production in the United States.

Application of biochar resulting from biomass pyrolysis has gained great interest recently as a bio-resource technology offering a variety of agricultural benefits, such as ameliorating soil quality, reducing fertilizer consumption, and sequestrating carbon (Lee et al., 2013). Biomass, a product of photosynthesis from carbon dioxide and water, is a valuable renewable resource available for energy (Lee et al., 2013) and durable soil amendment.

Biomass must be processed into biochar by a specific chemical reaction before it can be used: "At moderately high temperature in an inert atmosphere, pyrolysis thermally decomposes the carbohydrate structure of biomass into carbonaceous solid residue

(biochar), and condensable and non-condensable vapors of various molecular weight compounds" (Lee et al., 2013, p. 196).

The literature review indicates growing interest in application of biochar in sustainable soil improvement and carbon sequestration (Lehmann, Gaunt, & Rondon, 2006). Lehmann et al. (2006) suggested that producing biochar while producing energy from renewable fuels offers a potential for moving forward. "This potentially attractive combination means consumers can participate in an active carbon sequestration by using energy produced with the renewable and sustainable bio-char technology" (Lehmann et al., 2006, p. 422).

Use of biochar as a soil amendment could be traced back to the practices of ancient indigenous communities of the Amazon basin of adding low temperature wood charcoal to poor soils, creating the terra preta (found in Brazilian Amazonia), a very dark and rich in carbon soil with great productivity.

Reddy (2013) described the areas of application for biochar as manifold: "soil management, livestock, biomass energy, water purification, green habitats, sanitation and health" (p.1), and identified the ways in which biochar production creates value: energy creation, carbon sequestration, and creation of a valuable soil amendment.

Schmidt published "55 uses of Biochar," which summarized the variety of current applications of biochar (Schmidt, 2012). There are five areas of the application of biochar in the building sector: (1) insulation, (2) air decontaminations, (3) decontamination of earth foundations, (4) humidity regulation, and (5) protection against electromagnetic radiation. Among the variety of uses of biochar, the journal indicated the potential for its

use in construction as it has excellent thermal insulation capacities, low density, and an ability to mix with clay and portland cement. The two most valuable properties of biochar in the building sector are “its extremely low thermal conductivity and its ability to absorb water up to 6 times its weight” (Schmidt, 2012, p. 288). The literature review indicates that biochar offers many advantages for use in Green Buildings for raising the thermal insulation capacities of building materials and improve indoor air quality (Reddy, 2013; Schmidt, 2012).

According to Reddy (2010), biochar can be mixed in different proportions with cement, sand, earth, or other materials to produce brick, panels, or blocks. The literature review indicates that biochar is a good thermal insulation. Additionally, biochar has low density and absorbs $CO_{2;}$ it maintains a naturally constant level of indoor humidity between 45-70% during the summer and winter, which is the healthy range for indoor humidity, reducing the risks of allergies developing from moldy building materials, lowering the weight of the walls, and helping insulate walls (Schmidt, 2012). The biochar from different biomass, temperature, and properties has different properties and can be used for a variety of purposes. Applied as biochar plaster to exterior walls at a thickness of 20 cm, biochar is deemed a substitute for Styrofoam (Schmidt, 2012). The benefit to the building is twofold: the buildings become carbon sinks while improving the indoor climate. (Schmidt, 2012). Upon demolition, the biochar plaster can be recycled as a valuable soil additive (Schmidt, 2012).

Sustainability Concerns Related to Gypsum

Production of gypsum products involves temperatures not much higher than the boiling point of water, so the embodied energy of gypsum is relatively low, about 1200 BTU per pound for plaster and 2600 BTU per pound for gypsum board. The calcining process emits particles of calcium sulfate, which is an inert, benign chemical, as dust. The paper faces of gypsum board are made primarily of recycled newspaper. Some manufacturers produce gypsum board products made of as high as 95% recycled materials, including synthetic gypsum and recycled waste paper.

During the second half of the 20th century, the amount of construction and demolition (C&D) debris kept rising with the expansive trends of the construction industry. In an effort to help guide a program to recover construction materials, the Environmental Protection Agency (EPA) compiled data on C&D debris since 1998. Concrete, wood, and gypsum board comprised 65-95% of the C&D waste stream (Sandler, 2003). The 2003 EPA analysis showed C&D debris estimated by weight with gypsum board accounting for 5-15% of the estimated building related debris generated annually, ranking third after concrete and wood (Jeffrey, 2011). Currently, the European Union has revised their Waste Framework Directive to require 70% of their members state's C&D waste be reused or recycled by 2020 (Jeffrey, 2011). Canadian provincial governments also developed regulations to improve C&D waste recycling rates (Jeffrey, 2011).

Schultmann and Sunke (2007), noted that the construction industry in Europe was characterized by open-loop materials systems. With the significantly growing dumping

capacities of the construction industry and the limited land for landfills in Europe, the need to establish closed-loop materials systems in the building sector was determined to be vital. Schultmann and Sunke (2007) noted that despite the numerous existing recycling techniques for construction materials, the residential sector of the construction industry was in urgent need of innovation in regards to sustainability.

In 2013, U.S. domestic reserves of natural gypsum were considered adequate but not evenly distributed; gypsum cannot be substituted for the production of portland cement (US Geological Survey, 2014). Synthetic gypsum generated by industrial processes is an important substitute for mined gypsum. In 2013, synthetic gypsum accounted for about 43% of the total domestic gypsum supply (US Geological Survey, 2014). While naturally occurring gypsum is abundant, it is not renewable. The majority of newly extracted gypsum is quarried in surface mines, which can negatively affect the ecosystem bearing the risk of loss of wildlife habitat surface erosion and water pollution, in addition to the problem of disposing of overburden and mine tailings (Simmons, 2011).

An increase in the use of synthetic gypsum, material recovered from power plant flue gases that would otherwise end up in landfills, is a trend in gypsum construction materials. About 1.5 million tons of synthetic gypsum are used annually to produce approximately 7% of the U.S. construction industry's calcined gypsum. Some of the synthetic gypsum, however, contains toxic byproducts from the manufacturing processes and cannot be recycled into new construction materials. (Gypsum Association, via Simmons, 2011). As the production of synthetic gypsum from flue gas desulfurization

(FGD) continues, it will lead to a reduction in the mining of natural gypsum. However, availability of inexpensive natural gas may limit the increase of future FGD units.

The Declaration of Sustainability for biochar production determined three different ways biochar creates value as: a source for energy creation, means of carbon sequestration, and as soil amendment (Miedema & Flora, 2011). Over a dozen patents for biochar used as building material were issued in Asia (Schmidt, 2012). A lot of research was done on biochar's various applications in Asia, Africa, South America, and Europe. While biochar's applications in agriculture have been extensively studied, the literature review found no empirical research on testing biochar's thermal performance.

Disposal and Recycling of Gypsum

Gypsum board waste can be recycled back into manufacturing of new gypsum board products. Currently this amount is limited to 15-20% due to the amount of paper waste that can be safely introduced into gypsum without compromising the gypsum's fire resistance. Further, gypsum board waste from demolition of older buildings may be contaminated with lead-based paint, nails, or drywall tape joint compound, which need to be removed from the waste. These contaminants reduce the potential for recycling.

Gypsum board can also be used as soil amendments and plant nutrients. With the recent advent of mobile grinders, construction site recycling of gypsum board for agricultural purposes is more feasible. Gypsum is an ingredient in many manufacturing and industrial processes. Ongoing research is likely to find new potential uses of gypsum board waste (Simmons, 2011).

Gypsum is an inorganic material and, since gypsum board is primarily composed of gypsum, about 85-90% and only 7-15% paper, gypsum board cannot become compost. However, gypsum can be added after the compost has been created. Gypsum, though, can provide important nutrients to plants and has been used a soil amendment for centuries (EPA, 2012). According to the EPA's Waste Reduction Model (WARM) Version 12, gypsum board can be considered an additive to compost. The sources of gypsum board entering the waste stream are listed in Table 3:

Table 3

Composition of the Drywall Waste Stream

Source of Waste Drywall	% of Total
New Construction	64%
Demolition	14%
Manufacturing	12%
Renovation	10%

Source: EPA, 2012

CHAPTER 3

METHODOLOGY

Design

Due to the nature of the research the design of this study is truly experimental in nature. This study involved six groups of subjects: one control group of five samples which was 100% gypsum, and five experimental groups, containing five samples each, of biochar-gypsum mixes. The experimental groups were made of different percentages of biochar, ranging from 90% gypsum - 10% biochar to 50% gypsum - 50% biochar by volume.

The statistical analysis of the study was done with a one-way ANOVA with five levels, corresponding to the five experimental groups. Due to the limited time for experiments, the sample size was limited to thirty samples total. In the lack of previous empirical research on biochar insulation properties, a retrospective power study was conducted to validate the results.

This chapter provides an overview of the experimental research designed to determine whether the addition of corn stover biochar to gypsum affects the thermal conductivity, density, and flexural strength of the biochar-gypsum mixture. The researcher expected that with the increase of biochar content, the thermal conductivity, density, and the flexural strength of the composite would decrease.

Materials

The materials needed to make the control and experimental samples consisted of gypsum, biochar, and water.

Gypsum

A commercially available plaster of Paris dry mix, purchased from a Lowes store, meeting the ASTM C475 (ASTM International, 2014f) standard was used for this research.

Corn Stover Biochar

The corn stover biochar used in this study was a waste product of biofuel production through pyrolysis. Dr. ZhengRong Gu from the Agricultural & Biosystems Engineering Department at South Dakota State University provided the biochar for this study.

Water

Fresh cold tap water from Brookings, South Dakota, was obtained immediately before mixing, according to the instructions from Dr. N. Sai Bhaskar Reddy (Reddy, personal communication, June 7, 2016).

Preparation of the Biochar

Initially the dry granular biochar material was submerged under still water for two weeks. The water was replaced on daily basis, in June per instructions of Dr. Reddy (Reddy, personal communication, June 7, 2016).

The biochar was air dried for a week at ambient temperature and ground to pass sieve size #10 but not #20 (ASTM International, 2014a). The sieved biochar was then kept in a closed container in a temperature and humidity-controlled environment prior to the day of mixing. Figure 1 is a photograph of the prepared biochar and Figure 2 is a photograph of the Certified Sieves used.

Figure 1. Photograph of Prepared and Sieved Biochar-Size 20

Figure 2. Photograph of Sieves Used

Naming Convention of Tested Materials

Each sample in a group was given a number from 1 to 5, with a prefix of the type of material used.

Calibration materials: All of these products were commercially available -

Gypsum Board: 1/2” gypsum board

XPS: 2” Extruded Polystyrene

OSB: ½” oriented strand board.

P.100: The 100% gypsum samples prepared by the researcher as the control group.

P.90: The 90% gypsum-10% biochar samples prepared by the researcher as an experimental group. The naming convention was similar for the P.80, P.70, P.60, and P.50A experimental sample groups.

Note about the P.50A name: Some of the first batch of P.50 samples were broken during the unmolding process. The casting and molding process was adjusted, and the notation “A” in P.50A represents the second group of 50% gypsum-50% biochar samples that were made and tested.

Additionally, to measure and record the thermal conductivity of corn stover biochar, as a reference value only, samples named Biochar were prepared by the researcher. These samples were not a part of the control and experimental group statistical analysis.

Measurements Used During Sample Preparation

As seen in Table 4, the amount of gypsum and biochar needed to make the samples for the control and experimental groups were calculated and measured before the samples were mixed. The P.100 control group samples were made with dry gypsum and water only, per the manufacturer’s recommended mix of two parts gypsum to one part water. The P.90 samples were made with 3.5 cups of biochar and 31.5 cups of gypsum, to make 35 cups total of mixture (plus water) needed to make the 5 samples of the P.90

experimental group. Note that 3.5 cups of biochar is 10% by volume of the 35 cups total in the mixture.

Table 4

Experimental Mix Ratios by Volume

Material	Biochar		Gypsum		Water	
Mix	cups	grams	cups	grams	cups	grams
P.100	0	0	42	8135	21	5040
P.90	3.5	359	31.5	6110	15.75	3780
P.80	6	666	18	3493	9	2160
P.70	9.5	1062	22	4260	11	2640
P.60	16	1752	24	4653	12	2880
P.50 A	19	2050	19	3679	9.5	2280

Note: 1 cup = 1 U.S. legal cup = 0.24 liters (l)

To assure that the amount of material being prepared was correct, after each cup of material was added, the researcher measured the weight of the total mixture, using a Setra EL-4100S Model RS 232 scale, seen in Figure 3.

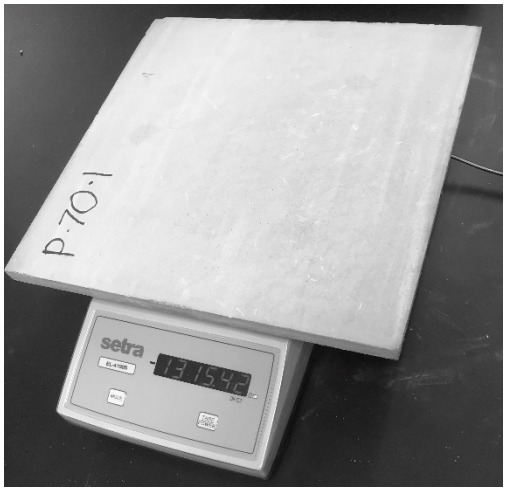

Figure 3. Setra EL-4100S Model RS 232 Scale

As an example, Table 5 is a record of the measurements for the gypsum portion of the P.50A samples, to assure that the correct of amount of gypsum was available before the biochar-gypsum mixture was combined. The gypsum weighed, as an average, a rounded value of 194 grams per cup (dry).

Table 5

Recorded Volume (Cups) and Weights (Grams) when Preparing the P.50A Sample's Gypsum Portion

Gypsum volume	Dry Weight	Calculated weight of 1 cup
cups	grams	grams
1	193	193
2	394	197
3	581	193.67
4	777	194.25
5	974	194.8
6	1154	192.33
7	1351	193
8	1543	192.88
9	1736	192.89
10	1941	194.1
11	2136	194.18
12	2326	193.83
13	2530	194.62
14	2745	196.07
15	2911	194.07
16	3110	194.38
17	3304	194.35
18	3493	194.06
19	3679	193.63

Average weight of 1 cup = 194.06 grams

The same procedure was followed in preparing the biochar for the P.50A group, with the results seen in Table 6. The biochar weighed, as an average, a rounded value of 110 grams per cup (as prepared by researcher).

Table 6

Recorded Volume (Cups) and Weights (Grams) Used when Preparing the P.50A Sample's Biochar Material

Biochar volume	Dry Weight	Calculated weight of 1 cup
cups	grams	grams
1	105	105
2	219	109.5
3	333	111
4	444	111
5	554	110.8
6	666	111
7	780	111.43
8	894	111.75
9	1007	111.89
10	1116	111.6
11	1216	110.55
12	1320	110
13	1424	109.54
14	1532	109.43
15	1637	109.13
16	1752	109.5
17	1859	109.35
18	1951	108.39
19	2050	107.89

Average weight of 1 cup = 109.93 grams

Mold Preparation

To assure the levelness and accuracy of dimensions of the samples, molds were constructed from birch plywood. Each side piece of the mold was secured to the base with metal screws, to allow for easy disassembly. The molds were made so all samples were a size of 12” x 12” x ½” (½” being the thickness of standard gypsum board for residential construction). The mold surfaces were cleaned, smoothed, and sealed against moisture with polyurethane prior to each casting. See Figure 4 for an overview of the molds, and Figure 5 for the measurement of the size of a typical sample.

Figure 4. Mold Forms for Casting Samples

Figure 5. Dimensions of a Typical Sample

Mixing and Preparing Specimens

On the day of mixing, ground and sieved biochar was measured by volume and weighed. Then the biochar was submerged in a still water bath for eight hours. Prior to mixing, only submerged material was collected and used immediately to mix with the

gypsum and cast in molds per instructions of Dr. Reddy (Reddy, personal communication, June 7, 2016).

Cold tap water, measured by volume, was added to biochar and mixed. Gypsum was added gradually and mixed at low speed for six to ten minutes, with an up-and-down motion using a hand-held drill, until a consistent mixture with no lumps was achieved (See Figure 6).

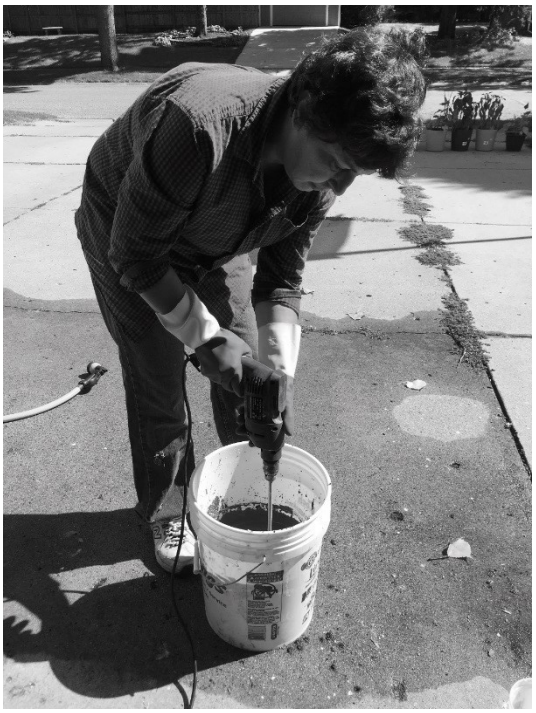

Figure 6. Mixing the Biochar-Gypsum Material

The mixture was cast in molds and leveled to the ½" thickness with a wood board to remove the excess mixture, and left in the mold to harden (See Figure 7).

The biochar-gypsum samples were removed from the molds within 24 hours, and then left to dry in a controlled indoor environment (humidity: 50-60%; temperature 72-74 °F) for a week, before measuring for density and testing for thermal conductivity.

Figure 7. Casting the Biochar-Gypsum Mixture into Molds

Hot Box Test Apparatus

A hot box apparatus, similar to the one used by Abu-Lebdeh et al. (2014), was manufactured and assembled to measure the thermal conductivity of the tested materials. This section discusses the equipment, connections, and calibration of the hot box apparatus; later sections provide more details on the thermal conductivity test procedure and measurement uncertainty and correction of measurement errors. Numbers in the

discussion (1 through 12) refer to the various construction, sensors, and test equipment used, as seen in Figure 8. The curved lines represent connecting cables of various types.

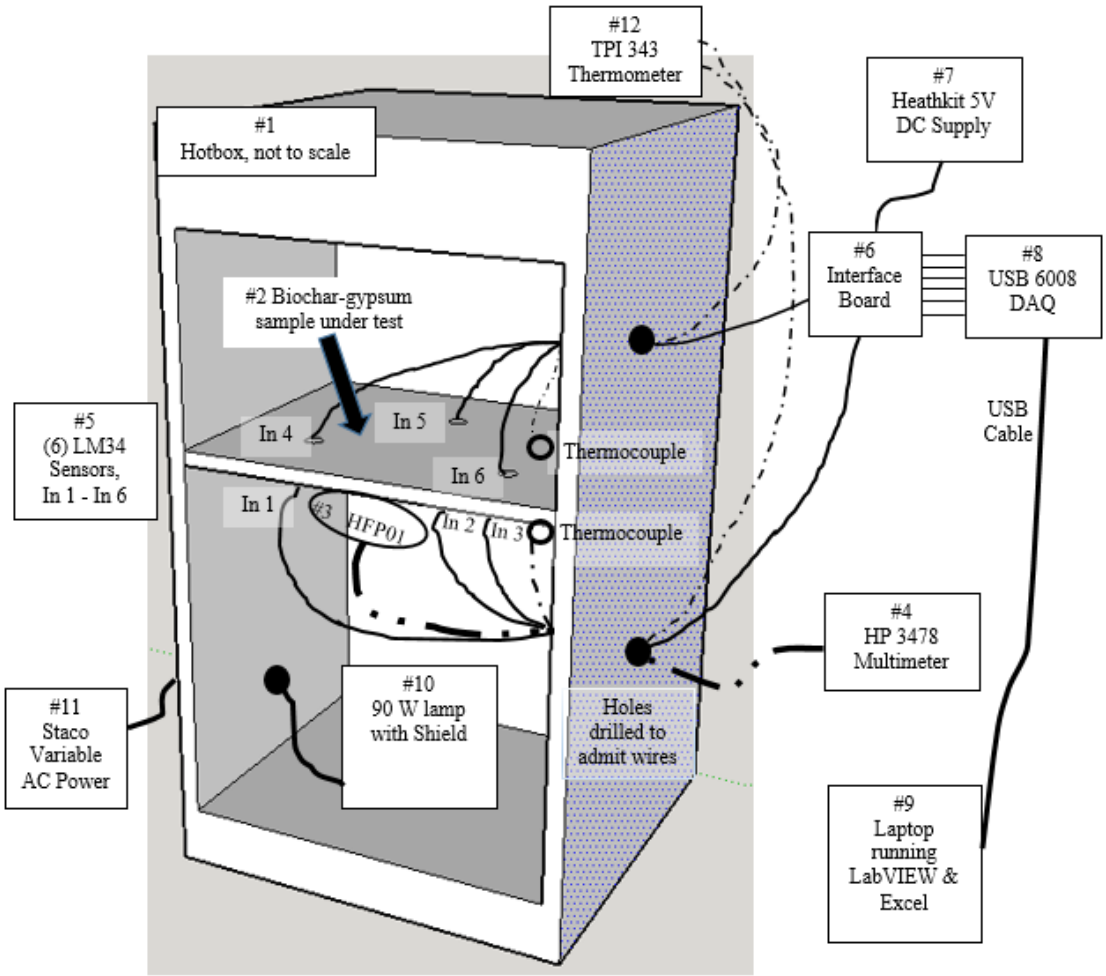

Figure 8. Hot Box Test Apparatus

1. Hot box. In order to minimize heat losses to its surroundings, the testing chamber was constructed of two-inch thick Extruded Polystyrene (XPS) meeting ASTM 236 (ASTM International, 2014d) with an R-value of 10, with the XPS placed between two layers of ¼” birch plywood. All materials for the hot box were fastened with heavy duty construction glue, instead of nails, to avoid thermal bridges.

The door was insulated with two layers of offset XPS, covered on the inside surfaces with reflective insulation, to reflect heat and provide a tightly sealed closure. The inside dimensions of the box were 12 ½” x 12 ½” x 35 ½” tall, with a ½” strip of wood on the left and right sides, in the middle of the height of the box, to support the samples. See Figure 9, for photographs taken during the construction of the hot box frame, and of the completed door.

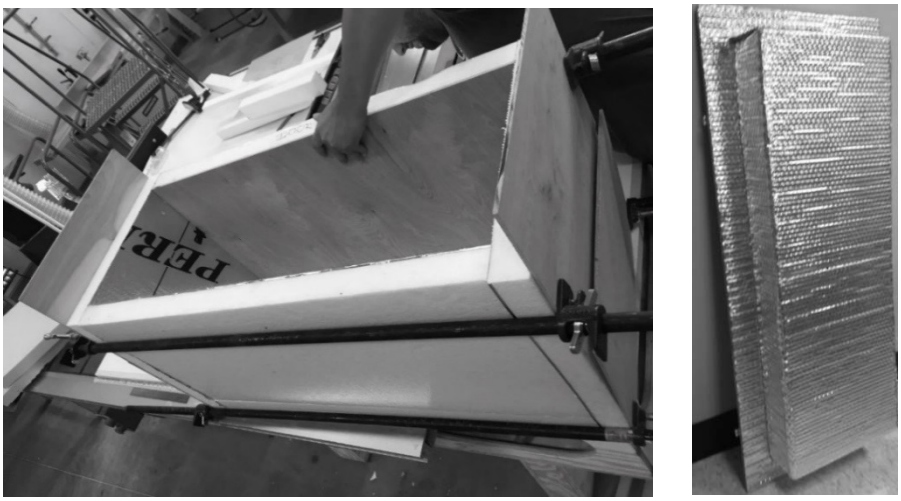

Figure 9. Hot Box Frame Construction and Completed Door

2. The control and experimental samples were placed on the wooden supports, and sealed along the edges with compressible insulation gaskets to reduce extraneous heat flow between the sample and the walls of the hot box.

3. HFP01 Heat Flux plate / Heat Flux Sensor from Hukseflux. The HFP01 served to measure the heat that flows through the object in which it is incorporated or on which it was mounted. Working completely passively, the HFP01 generates a small DC (Direct Current) voltage proportional to the local heat flux (Hukseflux Thermal Sensors, 2006). Figure 10 (Hukseflux Thermal Sensors, 2006) shows a schematic with dimensions of the sensor, as well as the location of the active sensor area and guard area.

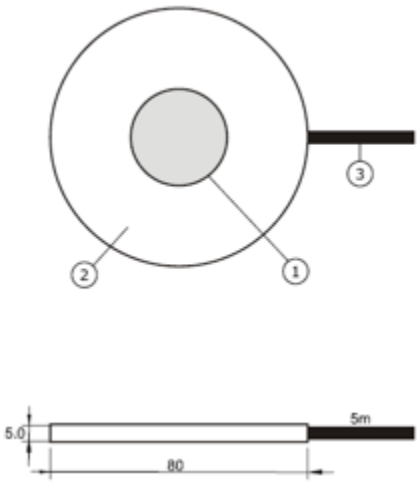

Figure 10. HFP01 Heat Flux Sensor Dimensions: Thickness 5 mm, (1) Sensor Area - approx 30 mm in diameter, (2) Guard Area of Ceramic-Plastic Composite outside of the Sensor Area – a total of 80 mm in diameter, and (3) Connecting Cable (Source: Hukseflux Thermal Sensors, 2006)

When mounting the heat flux sensor to the sample, air gaps were avoided as much as possible. As suggested by the HFP01 User Manual (Hukseflux Thermal Sensors,

2006), toothpaste was evenly spread over the mounting side of the sensor, to fill in any air gaps and assure consistent heat flow through the sensor and through the sample. The sensor was attached to the center of the bottom of the sample, see Figure 11, using standard heating and ventilation (HVAC) foil tape, as the tape had to hold the sensor up against the force of gravity. The tape overlapped the edge of the sensor by 10 mm at most. This was well inside the guard area, away from the sensor area, to avoid causing errors to the heat flux measurement.

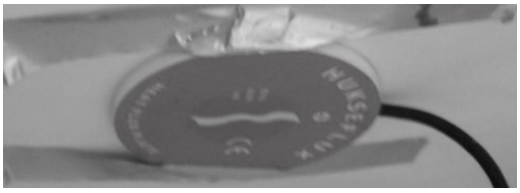

Figure 11. Attachment of HFP01 Sensor to the Bottom of the Biochar-Gypsum Sample

4. HP 3478A Multimeter, see Figure 12, was used to measure the voltage output of the HFP01 Heat Flux Sensor. The 3478A provides 5½ digit resolution for measuring DC volts. (Hewlett-Packard, n.d.) The multimeter displays the voltage generated by the HFP01 sensor, and that value was manually recorded by the researcher at specific times during the thermal conductivity test.

Figure 12. HP 3478A Multimeter

5. LM34 Precision Fahrenheit Temperature Sensors. The LM34 series devices are "precision integrated-circuit temperature sensors, whose output voltage is linearly proportional to the Fahrenheit temperature. The device can be glued to a surface and its temperature will be within about 0.02°F of the surface temperature" (Texas Instruments, 2016, p. 16). As shown on Fig. 8, a total of six temperature sensors were used, three on the bottom of the sample (In 1, In 2, and In 3), and three on the top of the sample (In 4, In 5, and In 6). The flat side of the LM34 sensor, see Figure 13, was attached to the samples with double-stick tape.

Figure 13. LM34 Temperature Sensor. (Source: Texas Instruments, 2016)

Wires were attached to each of the three legs of the sensor. The three wires were bundled together in cables, which were 2 meters long. The wires were attached on one end to the sensor, and on the other end to the interface board, and were wired to provide the sensor with:

1. +5 DC Volts to power the device

2. Ground connection

3. The voltage output signal to the input of the USB6008 DAQ, through the Interface Board.

The LM34 sensors were placed as pairs of temperature sensors directly across from each other. The sensors were placed 120° apart, at a minimum of 2.5” away from the edges of the sample and 2.5” diagonally from the HFP01 sensor. Figure 14 shows the bottom view schematic, with the attachment to a sample of all three LM34 sensors, and the HFP01 sensor, and Figure 15 is a photograph of the same, showing the foil tape and connecting cables.

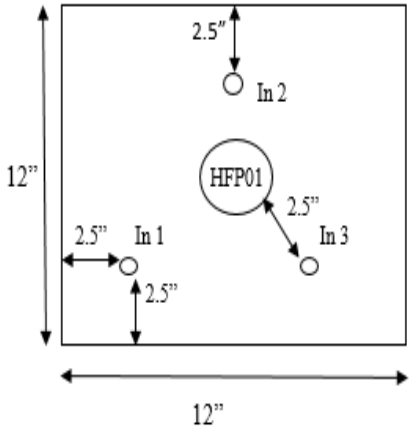

Figure 14. Schematic of the Bottom Side Connection of Sensors

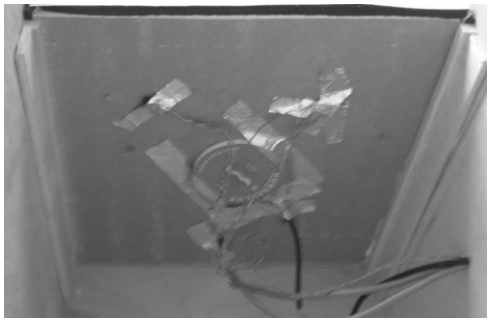

Figure 15. Photograph of the Bottom Side Sensors, Foil Tape to Attach the Sensors, and Connecting Cables

Figure 16 shows the top side schematic of all three LM34 sensors, and Figure 17 is a photograph showing sensors, adhesive tape and connecting cables. A much lighter tape, standard masking tape, was used on the top side to secure the sensors and cables.

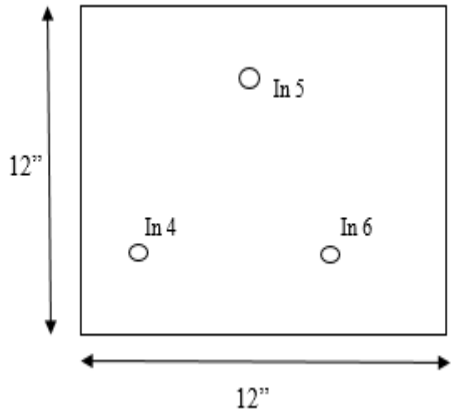

Figure 16. Schematic of Top Side Connection of Sensors

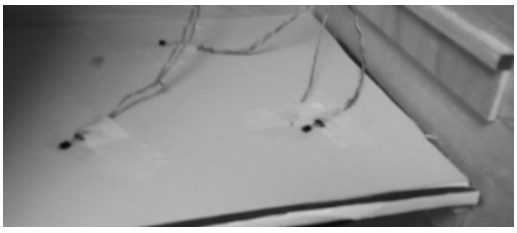

Figure 17. Photograph of Top Side Sensors, with Double-Sided Tape to Attach Sensors, Connecting Cables, and Masking Tape to Hold Cables in Place

6. Interface Board. Six sets of the 2-meter-long, three-wire, cables were soldered to a printed circuit board that provided an interface from the sensors to the USB6008 DAQ. See Figure 18 for the electrical connections schematic.

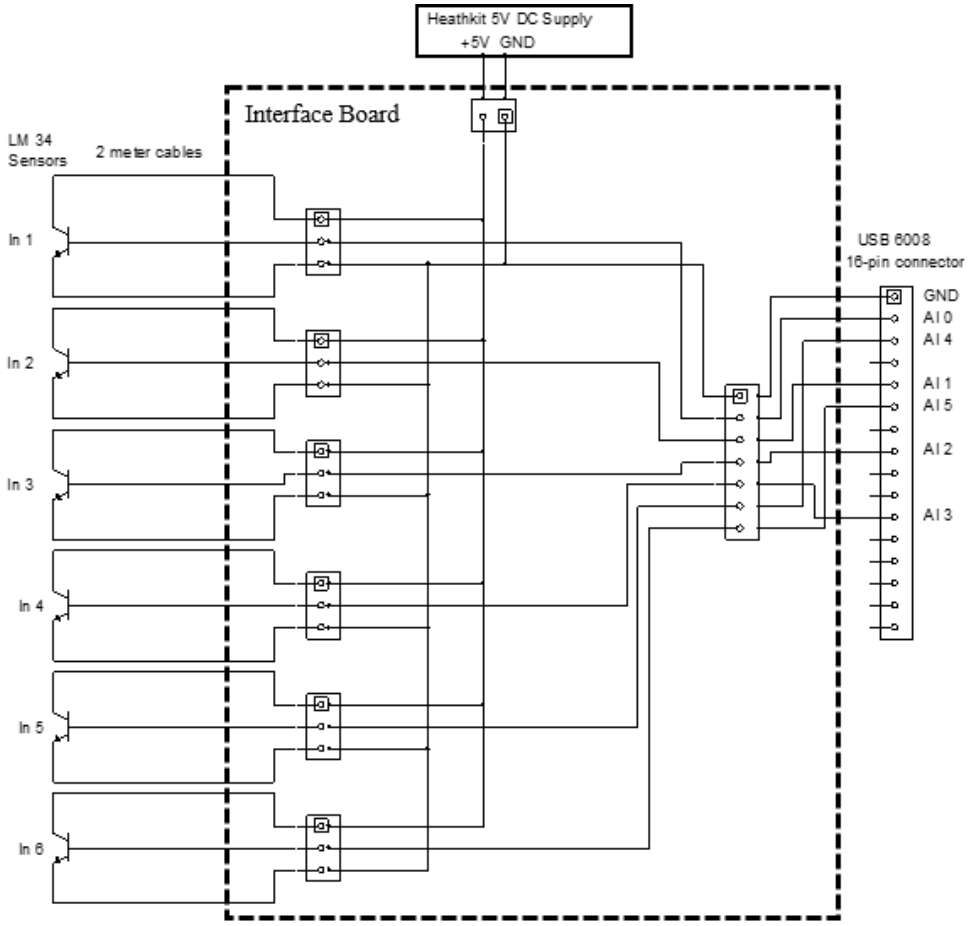

Figure 18. Interface Board Connections Schematic

7. Heathkit DC Power Supply to provide the +5 DC Volts used by the sensors, as seen in Figure 19.

Figure 19. Heathkit DC Power Supply

8. National Instruments USB6008 Multifunction DAQ (Data Acquisition) USB (Universal Serial Bus) Device. The USB6008 device provides eight single-ended analog input channels (National Instruments, 2015), as seen in Figure 20.

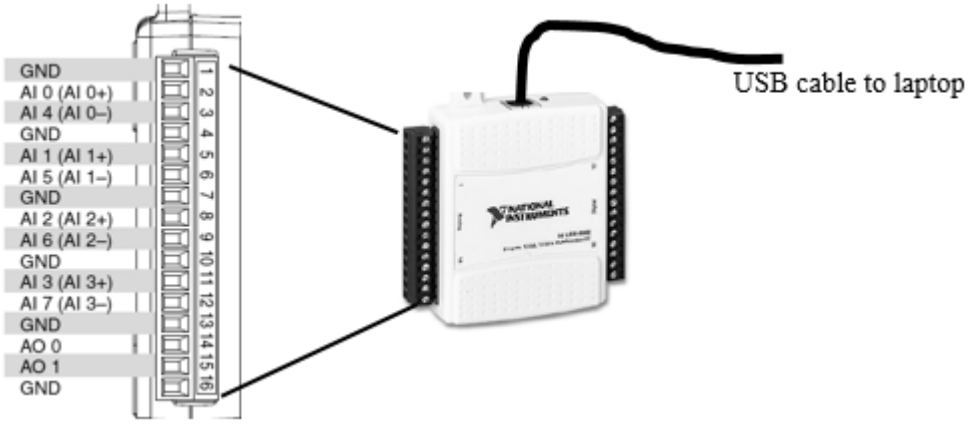

Figure 20. USB6008 DAQ Device and Input Channel Connections (Source: National Instruments, 2015)

9. Laptop with LabVIEW 2015 and Excel 2013 Software. A USB cable from the USB6008 DAQ to the laptop provides the digital information recorded from the LM34 temperature sensor readings to the LabVIEW software running on the laptop. See the Chapter 3 LabVIEW Programming section for details on the programming used in the thermal conductivity test procedure.

10. Heat source. A 90 W halogen lamp (light bulb), with an opaque panel on a stand above the light, so the lamp does not shine directly on the sample. As seen in Figure 21, the shield does not block the heat being generated in the hot side of the hot box.

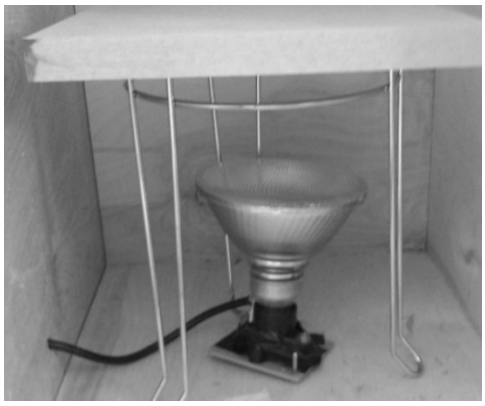

Figure 21. Heat Source Lamp and Shield

11. Staco Variable 120 Vac supply, where the halogen lamp is plugged in, as seen in Figure 22. One of the considerations of the hot box test procedure was to make sure that the active electronic sensors used did not exceed their maximum temperature ratings. The HFP01 sensor maximum temperature was +70 °C (Hukseflux Thermal Sensors, 2006) and the LM34 maximum temperature was 150 °C (Texas Instruments, 2016). As a result of preliminary tests, it was found that the variable power source needed to be set at 55%, to prevent the heat generated from exceeding the HFP01 sensor's maximum value in a two-hour test run. A separate power monitoring device was used, and it was found that the heat source lamp was using approximately 50 Watts of power during the test.

Figure 22. Staco Variable 120 Vac Supply

12. TPI 343 Dual Input K-Type Thermocouple Thermometer. The TPI contact temperature thermometer can be used with various Thermocouples; Type K, in this test. The thermometer has a resolution of 0.1 °C, a range of -50 °C to 1350 °C, and an accuracy of +/- 1.6 °C (Test Products International, 2016). It was used only to monitor the temperature difference across the sample in one place, and to help determine when the stabilized k value for the sample had been reached. Figure 23 shows the device, with two K-Type Thermocouples attach to the meter, and an entire Thermocouple cable assembly. The hot box test apparatus, with electronic test equipment, are shown in Figure 24.

Figure 23. TPI 343 Dual Input K-Type Thermocouple Thermometer, and Type K Thermocouple Cable Assembly

Figure 24. Overview of the Hot Box and Test Equipment in the Lab

LabVIEW Programming

As referred to in Figure 8, the hot box test apparatus includes a laptop with LabVIEW 2015 and Excel 2013 Software. A USB cable from the USB6008 DAQ to the laptop provided the digital information from the LM34 temperature sensor readings to the LabVIEW software running on the laptop. LabVIEW is an integrated development environment designed for a variety of measurement systems. It is flexible enough for many types of measurement applications (National Instruments, 2016).

The software being run on LabVIEW is visual-oriented, which allows for setup without an extensive knowledge of programming. Figure 25 shows the visual programming for the hot box test, which was displayed on the laptop screen during the thermal conductivity testing.

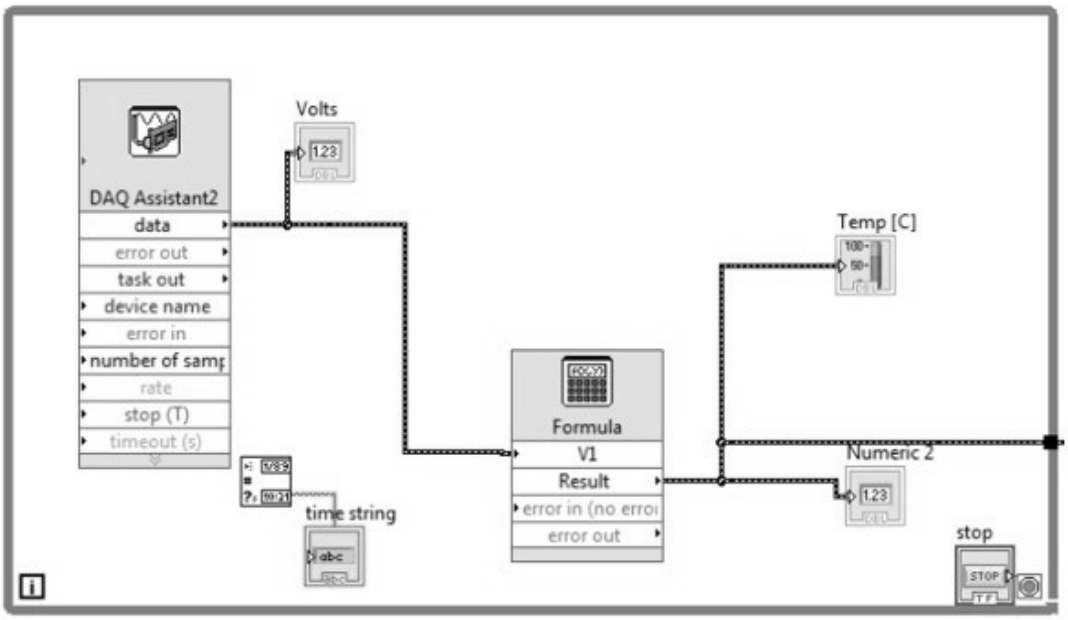

Figure 25. LabVIEW Programming for the Hot Box Test Apparatus

The “DAQ Assistant2” icon, as seen in Figure 25, was where specific programming instructions were recorded, and then those instructions were automatically sent to the USB6008 DAQ. First, it allowed for the setup of the USB6008 device inputs to be single-ended, with a maximum range of 5 Volts. Next, it programed, as seen in Figure 26, which input Channels (ai0 through ai5) were connected to the LM34 temperature sensors (In 1 through In 6).

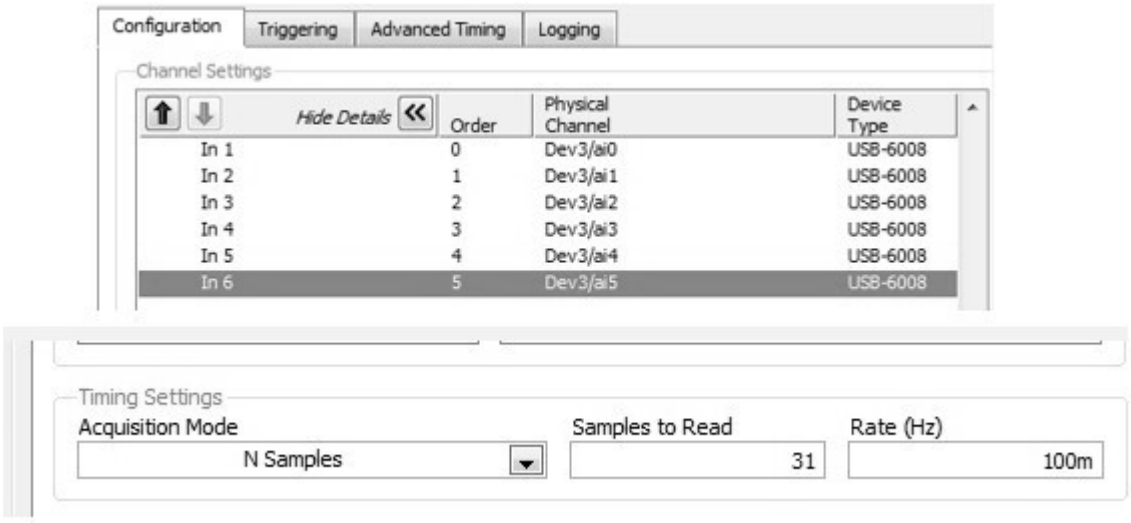

Figure 26. USB6008 DAQ Input Channel Definitions, under the DAQ Assistant2 Icon

The “DAQ Assistant2” icon was also used to determine when to capture data. The Logging Timing Settings, as seen in Figure 26, were set to capture data at a 100 mHz rate. This means that data was collected from all six sensors every 10 seconds (1/100 mHz). It also programs the software to record 31 “Samples to Read” each time through the program loop. Counting both the start time and end time of the loop, (31 samples) * (every 10 seconds) = 5 minutes. When one five-minute-long loop was completed, the

logging function generated and saved an Excel file, with the Voltage values from all six LM34 sensors, recorded every ten seconds.

The LabVIEW "Formula" icon in Figure 25 was the programming of the conversion factor of voltage to °C, used when the voltage gathered from the LM34 temperature sensor In 1, which was displayed during the test run.

The box around the icons of Figure 25 is the result of programming, a While Loop, where the software is programmed so that as soon as one five-minute-long data gathering loop was completed, the next loop starts immediately, within 10 mSec.

The "time string" icon in Figure 25 provided a value from the laptop's internal clock of the exact time that each set of data was recorded. See details on the procedure of running the thermal conductivity tests, and how Excel was used to record data, in the Chapter 3 Details of the Thermal Conductivity Measurement Test Procedure section.

Uncertainty of Measurements

In any measurement system, one has to consider the impact of several factors. The first was precision. In the field of instrumentation and electronic measurements, precision is "the repeatability of an instrument to record an identical output signal each time an identical input is applied" (Anthony, 2010, p. 121). Another consideration is accuracy, which is defined as "how close the measurement corresponds to its true value" (Anthony, 2010, p. 121).

According to Taylor (1997), if in a measurement system, all the uncertainties are independent and random, overall uncertainty can be calculated as follows:

$$\text{Percent Uncertainty} = \sqrt{\left(\frac{\delta x}{x}\right)^2 + \left(\frac{\delta y}{y}\right)^2 + \ldots} \qquad (1)$$

where, for each measurement device:

$$\text{Percent Uncertainty} = \frac{\delta x}{x} = \frac{\text{accuracy}}{\text{measurement value}} = \text{value in percent} \quad (2)$$

There were four sources of measurement uncertainty from the sensors and test equipment used in the hot box test apparatus:

1. HP 3478A Multimeter, used to measure voltage from HFP01 sensor. The multimeter specifications state for the 30 mV range, there is a 4½ digit readout, and there is a 1 μV (= 0.001 mV) accuracy (Hewlett-Packard, n.d.). When the thermal conductivity test procedure showed the k value had stabilized, there was a typical reading of 20 mV. So the measurement with the HP 3478A was considered to have an uncertainty of:

$$\text{Percent Uncertainty} = \frac{0.001\,\text{mV}}{20\,\text{mV}} = 0.005\% \quad (3)$$

2. LM34 Temperature sensors. The LM34 device provides typical accuracies of ±1½ °F over a full −50°F to +300°F temperature range (Texas Instruments, 2016). When the thermal conductivity test procedure showed the k value had stabilized, the hot side readings were approximately 140 °F and the cool side were approximately 120 °F, so an average of 130 °F can be used in the calculation of uncertainty for the LM34 temperature sensors:

$$\text{Percent Uncertainty} = \frac{1.5\,°\text{F}}{130\,°\text{F}} = 1.2\% \quad (4)$$

3. USB6008 from National Instruments (2015) was used to collect temperature values from the LM34 sensors, and then sent the values to the LabView program where they were recorded in an Excel file. This device has an accuracy of 4.28 mV (0.00428 V) (National Instruments, 2015). When the thermal conductivity test procedure showed the k value had stabilized, there was a typical reading of 1.3 V, so the USB6008 DAQ included an uncertainty of:

$$\text{Percent Uncertainty} = \frac{0.00428\,\text{V}}{1.3\,\text{V}} = 0.33\% \tag{5}$$

4. HFP01 Heat flux sensor from Hukseflux. The overall uncertainty statement according to ISO, is estimated to be within +5 /- 5% (Hukseflux Thermal Sensors, 2006), so the HFP01 sensor produced an uncertainty of:

$$\text{Percent Uncertainty} = 5\% \tag{6}$$

Considering these four devices of the hot box test apparatus, the entire test set-up has a total measurement uncertainty:

$$\text{Percent Uncertainty} = \sqrt{(5\%)^2 + (0.005\%)^2 + (1.2\%)^2 + (0.33\%)^2} = 5.2\% \tag{7}$$

This calculation shows that the majority of the uncertainty comes from the HFP01 heat flux sensor. The Chapter 3 Details of the Thermal Conductivity Measurement Test Procedure section explains how this measurement uncertainty was corrected for by averaging measurements over time.

Calibrating the Hot Box Test Apparatus

Calibration is "the process of adjusting an instrument or compiling a deviation chart (or equation) so that its reading can be correlated to the actual value being measured" (National Joint Apprenticeship and Training Committee, 2008, p.7). For this study, the calibration process measured materials that had a known, published thermal conductivity value, and then compared the measured values to the published values. From this, a correction factor, or calibration equation, was generated.

Specifically, the calibration procedure involved measuring the thermal conductivity value, k, for three different commercially-available, materials: ½" gypsum board, ½" oriented-strand board (OSB), and 2" Extruded Polystyrene (XPS). These samples were carefully cut so they were the 12" x 12" size that the hot box required. There were published insulation values (R value) for all three of these materials. Arch Media Group LLC (n.d.) said ½" gypsum board has R = 0.45 and XPS has R = 5 for 1", so R = 10 for the 2" material used in the test. Structall Building Systems (n.d.) gave a value of R = 0.62 for ½" OSB.

The units for R, in the U.S., are given in terms of (Square feet * degrees Fahrenheit * hour) per BTU:

$$\frac{ft^2 * {}^\circ F * hr}{BTU} \tag{8}$$

Values for thermal conductivity, k, have units of Watts per (meter *degrees Kelvin):

$$\frac{W}{m * Kelvin} \tag{9}$$

Note: In this study, the word Kelvin is spelled out, in order to differentiate it from the thermal conductivity symbol, k.

Hart, writing for Insulation.org (2009), explained the relationship between R and k as:

$$k = \frac{\text{thickness of material}}{R} \tag{10}$$

Taking into account the units used in the definitions of R and k, conversion factors gathered from RapidTables Online References and Tools (n.d.), and the relationship between R and k, the conversion of R = 0.45 to k for a ½" (0.0127 m) thick gypsum board was calculated by:

$$k = \frac{0.0127\ \text{m}}{\left(0.45 \frac{\text{ft}^2 * °\text{F} * \text{hr}}{\text{BTU}} * \left(\frac{\text{m}}{3.28\ \text{ft}}\right)^2 * \frac{\text{Kelvin}}{1.8\ °\text{F}} * \frac{3.412 \frac{\text{BTU}}{\text{hr}}}{\text{W}}\right)} = 0.160 \frac{\text{W}}{\text{m} * \text{Kelvin}} \tag{11}$$

This value agreed with the Gypsum Association (2010) value. That source gave the thermal property, in terms of R, of ½" (0.0127 m) gypsum board as 0.079 (Kelvin * m^2) / W. Converting to thermal conductivity, k, for ½" thick material:

$$k = \frac{0.0127\ \text{m}}{0.079 \frac{\text{Kelvin} * \text{m}^2}{\text{W}}} = 0.160 \frac{\text{W}}{\text{m} * \text{Kelvin}} \tag{12}$$

Similar conversions were made from R to k for the OSB and XPS materials. Table 7 gives the published values for R, and the converted values for thermal conductivity, k, for all three commercially available materials

Table 7

Values of R and k for Calibration Materials

Material – all commercially available	R-value $\left(\frac{ft^2 * °F * hr}{BTU}\right)$	Thermal conductivity, k $\left(\frac{W}{m * Kelvin}\right)$
½" Gypsum Board	0.45	0.160
½" OSB	0.62	0.116
2" XPS	10	0.0288

The hot box apparatus was set up, and tests carried out for four samples each of ½" gypsum board, ½" OSB, and 2" XPS. Table 8 gives the thermal conductivity values measured for each sample, along with each sample group's mean and standard deviation.

Table 8

Thermal Conductivity Data Gathered from Testing the Calibration Materials

Sample	k value Published	k value Measured	Measured Group Mean	Measured Std. Dev.
Gypsum Board #1	0.160	0.1662		
Gypsum Board #2	0.160	0.1612		
Gypsum Board #3	0.160	0.162		
Gypsum Board #4	0.160	0.1593	0.1622	0.00252
XPS #1	0.0288	0.0293		
XPS #2	0.0288	0.0343		
XPS #3	0.0288	0.0316		
XPS #4	0.0288	0.0327	0.03196	0.00182
OSB #1	0.1162	0.1067		
OSB #2	0.1162	0.1105		
OSB #3	0.1162	0.1065		
OSB #4	0.1162	0.1094	0.1083	0.00172

As seen in Table 9, for all three calibration material groups, the SPSS Shapiro-Wilk test returned a significance of 0.272 or higher, suggesting that the data collected for each group can be considered normally distributed.

Table 9

SPSS Shapiro-Wilk Test for Normality of the Calibration Test Data

	Shapiro-Wilk		
Material	Statistic	df	Sig.
XPS	0.990	4	0.959
OSB	0.863	4	0.272
Gypsum	0.934	4	0.618

Next, an SPSS Pearson Correlation was calculated, as shown in Table 10, with a result of R= 0.995, suggesting that the two paired variables of the published value and the measured value were strongly correlated, at a $p < 0.0001$ level, well within the $p < 0.05$ testing limit chosen for this study.

Table 10

Pearson Correlation for Calibration Materials

		k value published	k value measured
Pearson Correlation	k value measured	1.000	0.995
	k value published	0.995	1.000
Sig. (1-tailed)	k value measured		0.000
	k value published	0.000	

A linear regression line was generated in SPSS by producing a scatter plot, Figure 27, that shows the correlation coefficient, the data plotted, and the equation of the best fit line.

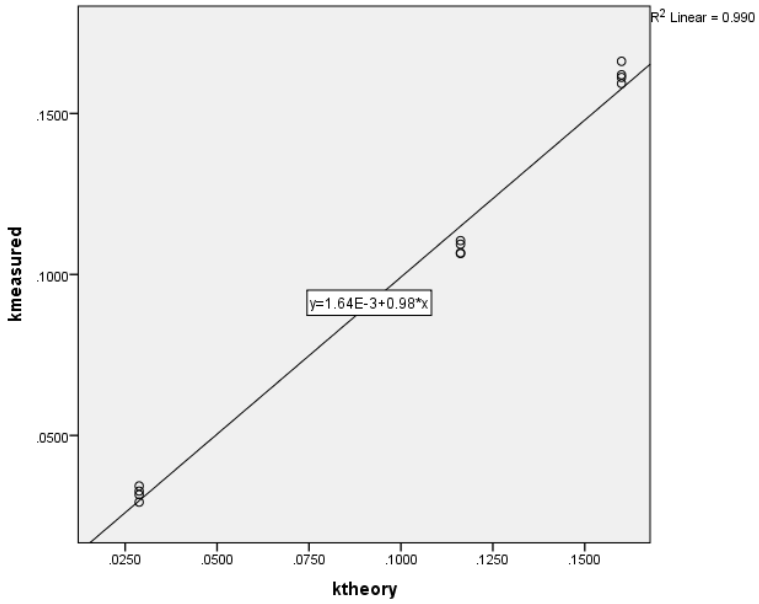

Figure 27. Scatter Plot and Calibration Equation for Hot Box Apparatus

This graph showed that the calculated linear equation fit the data with a correlation value of $R^2 = 0.990$, indicating a very good fit of the paired data to this linear equation. This regression equation is written as:

k value converted = 0.00164 + (0.98 * k value from hot box test) (13)

This was the correction factor that was applied to the data gathered from the hot box apparatus test of the control group and experimental group's samples created for this study.

Summary of Thermal Conductivity Test

The hot box test apparatus measured the heat flux through samples, which follow Fourier's Law

$$Q = - k \frac{\Delta T}{x} \quad (14)$$

where

Q = Heat flux, measured in $\frac{W}{m^2}$

ΔT = Temperature difference across the material section, in Kelvin (degrees Kelvin). As a practical aspect, the calculation used °C (degrees Celsius), which was numerically the same as degrees Kelvin.

x = Material thickness in m (meters)

k=Thermal conductivity in W/m-Kelvin

The hot box measurement apparatus produced values for Q and ΔT, and before each test the thickness of the sample x was measured, and the equation was rearranged so a value could be calculated for thermal conductivity, k:

$$k = -\frac{Q\,x}{\Delta T} \qquad (15)$$

Four of the main considerations of how the k value was measured and calculated are summarized here.

1. Many preliminary hot box tests were run on the calibration materials, and it was determined that the hot box test needed to run for 90 to 110 minutes, in order to achieve a stabilized k value for the sample. Specific rules were determined and followed as the tests on the samples were run.

2. There were three sets of temperature sensors placed on either side of the sample, as seen in Figures 14 and 16. A k value was calculated at each of those three

locations, and then an average of the three values was calculated, and used as the k value for the sample at the time those temperatures were measured.

3. To overcome the uncertainty of the measurements, particularly from the HFP01 sensor, measurements were made, and k values were calculated and recorded, every 5 minutes during the test. When it was determined, by monitoring the data being gathered by the test, that the k value was stabilized, the test was terminated. The last five calculations of k (collected over time) were averaged to produce the preliminary k value for the sample. That is, the uncertainties of the measured values, which were assumed to be random (some larger, and some smaller, than the true value), when averaged over time, produced a more accurate k value.

The procedure of averaging the k value over time for each sample was used in calibrating the hot box apparatus with the manufactured ½" gypsum board samples. The test procedure produced a k value for each sample that was at most 3.9% away from the published k value, as seen in Table 11. This gave the researcher a high degree of confidence that the test procedure, and the averaging-over-time calculation, was valid.

Table 11

Hot Box Apparatus Measurements of Manufactured Gypsum Board Compared to the Published Value

Sample	k value Published	k value Measured	Percent error from published value
Gypsum Board #1	0.160	0.1662	+3.9%
Gypsum Board #2	0.160	0.1612	+0.75%
Gypsum Board #3	0.160	0.1620	+1.25%
Gypsum Board #4	0.160	0.1593	-0.44%

4) As the final step in the calculation of k value for the samples, the hot box apparatus calibration correction factor was applied to the time-averaged preliminary k value. This resulted in the k value for that sample used in the statistical analysis of thermal conductivity.

Thermal Conductivity Measurement Test Procedure

The hotbox measurement apparatus produced values for Q and ΔT, and before each test the thickness of the sample x was measured, and therefore the equation to produce a k value, thermal conductivity, was:

$$k = -\frac{Q * x}{\Delta T} \tag{16}$$

The value of Q came from the HFP01 heat flux sensor, which provides a reading in milliVolts (mV), which must be converted to a value of W/m^2 (Hukseflux Thermal Sensors, 2006). For this study, a new HFP01 sensor was purchased. At Hukseflux, each sensor is given a factory calibration that provides the sensor conversion factor needed, before being shipped to the customer. See Appendix B for the calibration certificate from Hukseflux. For the HFP01 sensor used in the study, this conversion was

$$Q\,(W/m^2) = \frac{Vreading\,(mV)}{0.0617\ mV / (W/m^2)} \tag{17}$$

With these equations and conversion factors taken into account, an equation was used to calculate a k value from the data collected from the hot box test apparatus:

$$k = -\left(\frac{\frac{(HFP01\ \ reading\ in\ mV)}{0.0617} * (thickness\ \ of\ sample)}{\Delta T\ reading\ from\ \ LM34\ \ Temperature\ Sensors} \right) \tag{18}$$

As detailed in the hotbox setup section, the six LM34 temperature sensors were each connected to a channel in the USB6008 DAQ. The USB6008 device was sensitive enough to capture the milliVolt readings from the LM34 temperature sensors, but was not sensitive enough to capture the microVolt (0.001 milliVolt) values provided by the HFP01 heat flux sensor. This level of sensitivity required the use of the HP3478 Multimeter, which did not have an automatic voltage output that was compatible with the USB6008 interface to LabVIEW. Instead, readings from HP3478 Multimeter, were manually recorded by the researcher every five minutes during the hotbox test runs. The LabVIEW software recording was started exactly at the top of a minute as provided by the laptop used in the data collection, and a time stamp was saved. A hand-held stopwatch was used to ensure that readings from both the HFP01 heat flux and the temperature sensors were synchronized.

The following paragraphs refer to Table 12, and show the recorded measurements input to the Excel file, and calculations results used to find when the k value had stabilized for an example, sample P.100.4.

Table 12

Example of Data Recording and Calculation Process for P.100.4 Sample - Monitoring k and Terminating the Test when k Value is Stabilized

A	B			C	D	E
	TPI			HFP01		
	Manually recorded, to monitor the approx. results			Manually recorded	Manual estimate	
time stamp	Thot	Tcold	ΔT	mV	k	% change
5:45:00	24.5	24.4	0.1	0.0012	NA	NA
5:50:00	31.5	26.1	5.4	-19.188	0.7314	NA
5:55:00	34	27.5	6.5	-21.921	0.6942	5.09%
6:00:00	36.7	29	7.7	-23.262	0.6218	10.42%
6:05:00	39.2	30.7	8.5	-23.437	0.5675	8.73%
6:15:00	43.4	33.7	9.7	-23.185	0.492	13.31%
6:25:00	47.3	36.5	10.8	-23.285	0.4438	9.80%
6:35:00	50.7	39.1	11.6	-23.465	0.4164	6.18%
6:45:00	54	41	13	-23.08	0.3654	12.23%
6:55:00	56.5	43	13.5	-23.286	0.355	2.84%
7:00:00	57.3	43.9	13.4	-23.26	0.3573	-0.63%
7:05:00	58.7	44.6	14.1	-22.998	0.3357	6.04%
7:10:00	59.3	45.9	13.4	-23.167	0.3559	-6.00%
7:15:00	60.3	46.6	13.7	-23.072	0.3466	2.59%
7:20:00	61.2	47.1	14.1	-22.675	0.331	4.51%
7:25:00	62.3	48.3	14	-22.866	0.3362	-1.56%
7:30:00	62.9	48.9	14	-22.566	0.3318	1.31%
7:35:00	63.8	49.7	14.1	-22.548	0.3292	0.79%

Table 12, column A shows the laptop's time stamp value, which was recorded every five minutes. Note: As shown in Table 12, the data of the every 5 minutes was recorded at the start, to make sure that test run was recording properly. In the middle of the test run, before the k value was stabilized, the data only recorded every 10 minutes. Toward the end of the test run, the data was recorded every 5 minutes again. The time stamp row of 5:45:00 shows the conditions at the start of the test run, that the temperature

of the sample was at approximately 24.5 °C ≈ 76 °F on both the hot and cool sides, and that there was essentially no heat flux through the sensor. This test was conducted from 5:45:00 PM to 7:35:00 PM.

Table 12, column B showed the results of manual readings from the TPI Thermocouple Thermometer. These values were combined with the HFP01 readings of Table 12, column C that were also being manually recorded, and gave a sense of when the hotbox apparatus had produced a stabilized value for thermal conductivity. Note in Table 12, column D that the first k value calculated (timestamp 5:50:00) was 0.7314, and that the value decreased by large amounts every 5 minutes. The test had to run for an hour before the k value was even within 10% of the final value.

Table 12, column D was this manual estimate of k at each time recorded, for example k = 0.3292 at timestamp 7:35:00 (the bottom) of column D, calculated from the

- -22.548 from the heat flux sensor, bottom of column C
- 0.0127 m sample thickness estimate
- 14.1 Kelvin = ΔT from the TPI sensors, bottom of column B

$$k = -\left(\frac{\frac{(-22.548)}{0.0617} * (0.0127\ \text{m})}{14.1\ \text{Kelvin}} \right) = 0.3292\ \frac{\text{W}}{\text{m} * \text{Kelvin}} \qquad (19)$$

Table 12, column E is the calculated percent change from one calculation of k to the next, as a percent difference from the preceding value. The tests were planned to run approximately 90 minutes in order to achieve a stabilized k value (see that this sample

test was conducted for 110 minutes). The rules used to decide when the k value had stabilized were:

1. Three consecutive values of k, as measured and recorded in column D, had a change of less than 1%, or

2. Three consecutive values of k had a change of less than 2%, with one of the values being opposite in sign.

As the thermal conductivity test was conducted, the LM34 temperature sensors voltage values recorded by the USB6008 DAQ were saved with LabVIEW software into the Excel file. The LM34 temperature sensors were designed to produce a temperature value °F = 100 * voltage measured, so a conversion to °C was needed:

$$\text{Temperature °C} = ((\text{Voltage measured} * 100) - 32) * 0.5555 \quad (20)$$

Note: These Excel file columns with temperature sensor voltage values and conversions to °C were left out of this description in order that the tables fit on the paper.

Table 13 is a continuation of the Excel file shown in Table 12. The first two columns, A and C, are copies of columns A and C from Table 12. The temperature sensors were mounted on the samples in pairs, and values of ΔT of each pair were calculated. Pair 1, shown in Table 13, column F, was the difference, ΔT, between sensors In 4 and In 1. Pair 2, column H, were the differences between the In 5 and In 2 temperatures. Pair 3, column J, was the difference between the In 6 and In 3 temperatures.

Table 13

Example of Data Recording and Calculation Process for P.100.4 Sample - Calculation and Averaging

A	C	F	G	H	I	J	K	L	M
time stamp	HFP01 mV	ΔT, Pair 1 **In4-In1**	thick 0.01275 kpair1	ΔT, Pair 2 **In5-In2**	thick 0.0125 kpair2	ΔT, Pair 3 **In6-In3**	thick 0.0125 kpair3	Average of 3 kpair values	Average of last 5 time values
5:45:00	0.0012	NA	NA	NA	NA	NA	NA	NA	
5:50:00	-19.188	4.14	0.9584	9.3	0.4181	6.71	0.568	0.652	
5:55:00	-21.921	6.4	0.7075	10.43	0.4259	8.41	0.5177	0.5539	
6:00:00	-23.262	7.54	0.6379	12.12	0.3887	10.11	0.457	0.4976	
6:05:00	-23.437	8.1	0.5977	12.12	0.3917	11.24	0.414	0.4706	
6:15:00	-23.185	9.24	0.5187	13.25	0.3545	12.38	0.372	0.4176	0.5184
6:25:00	-23.285	9.24	0.5209	13.81	0.3415	12.94	0.3571	0.4089	0.4697
6:35:00	-23.465	10.37	0.4676	14.38	0.3306	13.51	0.3448	0.3833	0.4356
6:45:00	-23.08	10.37	0.4599	14.94	0.3129	14.08	0.3254	0.3683	0.4098
6:55:00	-23.286	10.94	0.4399	16.07	0.2935	14.08	0.3283	0.3561	0.3869
7:00:00	-23.26	10.94	0.4394	15.5	0.3039	14.65	0.3152	0.355	0.3743
7:05:00	-22.998	10.94	0.4345	15.5	0.3005	14.65	0.3116	0.351	0.3628
7:10:00	-23.167	10.37	0.4615	15.5	0.3028	14.65	0.3139	0.3615	0.3584
7:15:00	-23.072	11.51	0.4144	16.07	0.2909	14.65	0.3126	**0.3414**	0.353
7:20:00	-22.675	11.51	0.4072	16.07	0.2859	14.65	0.3072	**0.3355**	0.3489
7:25:00	-22.866	10.94	0.4319	16.63	0.2785	14.09	0.3222	**0.3464**	0.3472
7:30:00	-22.566	11.51	0.4053	16.06	0.2846	14.09	0.3180	**0.3381**	0.3446
7:35:00	-22.548	11.51	0.4049	16.06	0.2844	14.66	0.3117	**0.3337**	**0.3390**

The value of x, the thickness of the samples, was nominally ½" = 0.0127 meters. As the samples were produced, it was noted that the thickness was not exactly ½" at all places of the sample, and the k calculation was very sensitive to an accurate value of thickness, x. To take this variation into account, each sample was measured at the edge in the middle of each of the four sides, and better estimates were obtained of the sample thickness at the location where the LM34 temperature sensors were located. For example, for sample P.100.4, Figure 28 shows the edge thickness measurement in the middle of each side, *in italics*. Sensor Pair 1 is midway between the left side and front measurement values of 13 mm and 12.5 mm, giving an improved estimate of the thickness where the

sensor is located as 12.75 mm, marked with a parenthesis. Sensor Pair 2 is close to the back measurement, so that measurement of 12.5 mm is used. Sensor Pair 3 is midway between the right side and front measurements of 12.5 mm and 12.5 mm, giving a value of 12.5 mm used in the calculations.

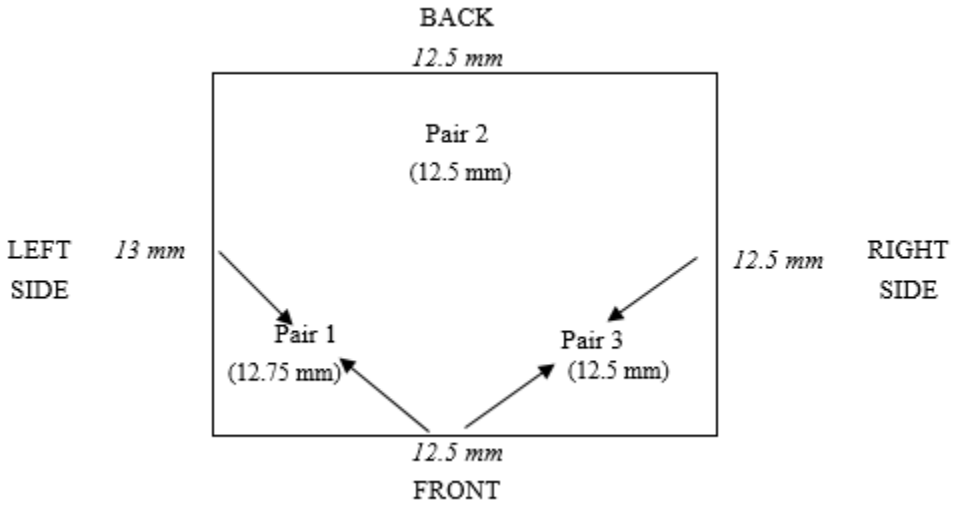

Figure 28. P.100.4 Sample Thickness Measurements, in Italics, and Estimates of Sample Thickness, in Parentheses, for the LM34 Temperature Sensor Pairs

Each pair of ΔT difference values was used to calculate a k value for that specific area of the sample. The thickness measurements, as noted at the tops of Table 13 columns G, I, and K, were used in the calculation of k at each temperature sensor pair location. See Appendix C for the measurements and calculations for the thickness of all 5 control and 25 experimental samples measured.

At each sensor pair location, a k value was calculated, for example at the bottom of column K, at time stamp 7:35:00, using the values of

- -22.548 mV from the heat flux sensor, bottom of column C
- 0.01250 m thickness, top of column K

- 14.66 Kelvin temperature difference of Pair 3, bottom of column J

$$k = -\left(\frac{\frac{(-22.548)}{0.0617}\frac{W}{m^2} * (.01250\ m)}{14.66\ Kelvin} \right) = 0.3117 \frac{W}{m * Kelvin} \quad (21)$$

This process produces three values of k at three different places on the sample. Column L was an average of the three k values from Table 13 columns G, I, and K, producing a k value = 0.3337 W / (m * Kelvin) at timestamp 7:35:00.

As the heat flux sensor was measuring a value that has significant digits down to 0.001 milliVolts, electrical noise can cause major difficulties in this measurement system. That is in addition to the approximately 5% uncertainty that is present in the heat flux sensor measurement value at any one time. To overcome these possible sources of error, it was decided that the final k value calculated for the sample would be an average of the last five time-stamped k calculations, averaged over time, which was calculated in column M. This method helped cancel out any random errors that were present. For the P.100.4 sample, this calculation included the bolded values in Table 13:

$$k\ average = \frac{0.3414 + 0.3355 + 0.3464 + 0.3381 + 0.3337}{5} = 0.3390 \frac{W}{m * Kelvin} \quad (22)$$

Note, as shown in Table 14, the last five k values over time were all within 2.2% of the average value, but varied (some above, and some below) the averaged value. This result was expected due the design of the hot box apparatus, and the uncertainty present

in the sensors and test equipment. This result reinforced the decision to implement the time-averaging process, to offset that source of error.

Table 14

Last Five k Values Calculated in the Example Test Run, Showing the Effect of the Uncertainty in Measurements

Timestamp	k value calculated	Percent error from average of last 5 readings (0.3390)
7:15:00	0.3414	+0.70%
7:20:00	0.3355	-1.00%
7:25:00	0.3464	+2.20%
7:30:00	0.3381	-0.20%
7:35:00	0.3337	-1.60%

Finally, the hot box calibration correction factor, see equation 13, was applied to the time-averaged value:

$$k = 0.00164 + (0.98 * 0.3390) = 0.3339 \ \frac{W}{m * Kelvin} \qquad (23)$$

This k value = 0.3339, was the value used as the measured value of thermal conductivity for the P.100.4 sample. This procedure was used for the five control samples and the twenty-five experimental biochar-gypsum mixtures, and for the biochar-alone in the "glass panel" measurements.

Test Procedure for Thermal Conductivity of Biochar

Due to the lack of experimental research of biochar's thermal conductivity, it was decided to measure the thermal conductivity of the biochar used in this study, corn stover ground to pass sieve size #10 but not #20. At 100% concentration, the biochar cannot be

formed into a solid panel that could be tested in the hotbox apparatus without adding some stiffening material, which would affect the thermal conductivity overall. The solution was to make a glass-biochar panel with loose biochar suspended between panes of glass (with known k value) on the top and bottom. The glass was separated by ½" x ½" wooden spacers around the outside edge. See Figure 29 for the measurements, and Figure 30 for a photograph, of the glass-biochar panel.

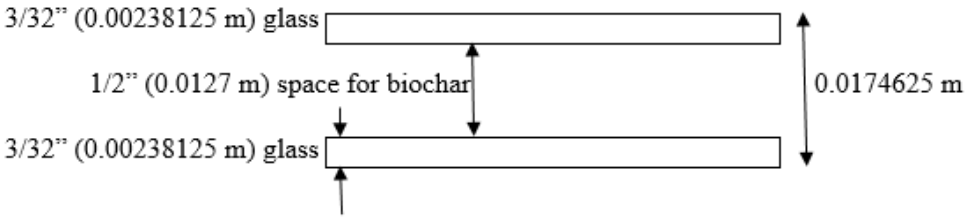

Figure 29. Side View Schematic of Glass-Biochar Panel

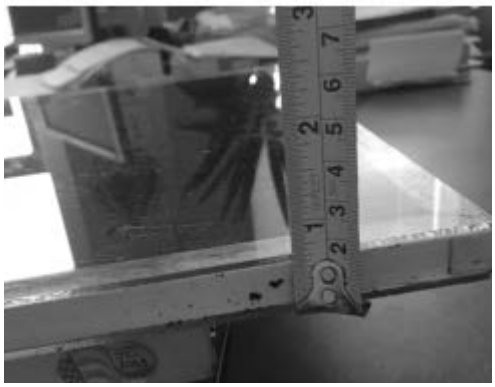

Figure 30. Side View Photograph of Glass-Biochar Panel

The R-value of a structure with multiple layers was the sum of the R of the individual layers. The glass in the panel added its own (small) insulation value to that of

the biochar. According to The Engineering Toolbox (n.d.), window glass has a thermal conductivity value, k = 0.96 W/ (m * Kelvin).

This means for the 3/32" glass the test used, each pane of glass had an R value:

$$R = \frac{\text{thickness}}{k} = \frac{0.00238125\ \text{m}}{0.96\ \frac{\text{W}}{\text{m} * \text{Kelvin}}} = 0.00248\ \frac{\text{m}^2 * \text{Kelvin}}{\text{W}} \qquad (24)$$

For both panes of glass:

$$Rglass = 2 * \left(0.00248\ \frac{\text{m}^2 * \text{Kelvin}}{\text{W}} \right) = 0.00496\ \frac{\text{m}^2 * \text{Kelvin}}{\text{W}} \qquad (25)$$

For the glass-biochar panel as a whole, R is found by using the hotbox measurement of values for Q and ΔT, referring back to Equations 9 and 10:

$$R = \frac{\text{thickness (x)}}{k} = \frac{x}{\frac{Q * x}{\Delta T}} = \frac{\Delta T}{Q} \text{ in units of } \frac{\text{m}^2 * \text{Kelvin}}{\text{W}} \qquad (26)$$

In the hotbox apparatus, the pairs of temperature sensors, placed directly across from each other in three different places, produced the values of ΔT, and Q is measured in one place with the HFP01 sensor. Each temperature difference was used to calculate a value of R at that spot

$$R = \frac{\Delta T}{Q} \qquad (27)$$

The three different values of R averaged to produce an R value for the glass-biochar panel. Then the R value for the glass is subtracted to find the R of the bulk biochar alone.

$$R_{biochar} = R_{panel} - R_{glass} \quad (28)$$

Density Calculation of Control and Experimental Samples

In addition to testing thermal conductivity and flexural strength, this study measured the density of the P.100 control group and the P.90 – P.50A experimental group's samples.

Each sample was weighed, to the nearest gram, with the Setra EL-4100S Model RS 232 scale. The scale has a measurement accuracy to +/- 0.01 grams (Setra Systems, 1998). The length and width of each sample was measured. To counter the effect of possible variations in thickness across the sample, due to the nature of the casting process, samples were measured on the edge, in the middle of each side, and an average of the four readings was calculated. This value was used for the thickness value. See Appendix D for the measurements and calculations of density for all five control samples and all twenty-five experimental samples. The calculation of density was:

$$\text{density}\left(\frac{g}{cm^3}\right) = \frac{\text{weight (in grams)}}{\text{length} * \text{width} * \text{thickness (all in cm)}} \quad (29)$$

Flexural Strength Testing of Control and Experimental Samples

The flexural properties of the control and experimental samples were evaluated following the ASTM C473-12 standard (ASTM International, 2014e) by supporting the 12" by 12" specimen symmetrically, 2" away from the edges, and applying a transverse load midway between the supports. The supports were placed 8" apart, with the edge

rounded (R = 0.125”) so as to not pierce the specimen, following the ASTM C473-12 standard. The load bar on top was in contact with the full width of the specimen, and was midway between the bottom-side supports. This was so the center of the load-bearing surface passed through the specimen at one-half of the specimen width and one-half of the distance between the supports. See Figure 31 for details. Also specified by the ASTM C473-12 standard was the speed that the downward plate, the flexural force, was applied to the sample, and for this test that was set at 1” / min.

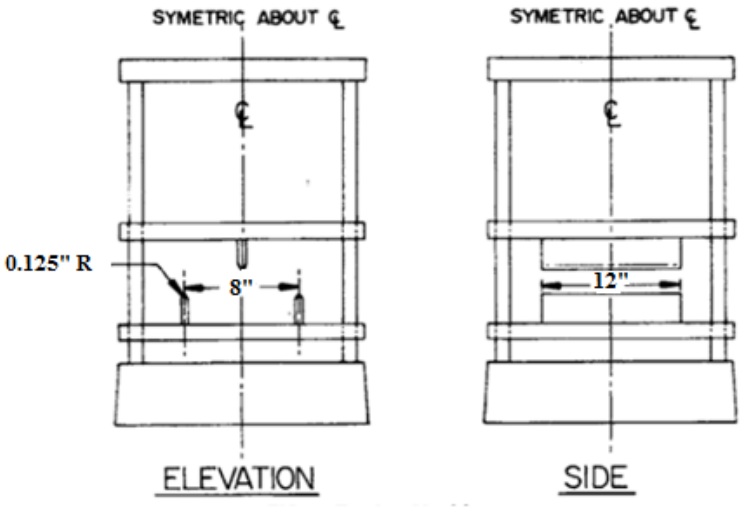

Figure 31. ASTM C473-12 Flexural Test Machine, Modified From the ASTM Standard to Fit the Sample Sizes Used in the Study. (Source: ASTM International, 2014e).

The test fixture was modified from the ASTM standard, because the samples were 12” x 12” in size, different than what the standard called for, and so the distance between the lower supports was reduced from the ASTM standard 10” down to 8”.

The test measured flexural strength by determining the load, in Newtons (N), at the time of a transverse failure through the thickness of the specimen (the specimen

breaks through completely). The flexural strength of the experimental group mixtures were compared with the control group.

All flexural strength experiments were conducted at the Materials Testing Lab (South Dakota State University, 2016), South Dakota State University, Brookings, South Dakota, using the MTS Insight 5 Material Testing System. This system used a precision DC Servo motor and was capable of 2 kiloNewton (kN) of force, with a range of test head speed of 0.00012” / min to 100” / min (MTS Systems Corporation, 2007). The force being applied was measured by an MTS 661.20 Force Transducer, with a measurement precision of 0.005 Newtons (MTS Systems Corporation, 2016). Figure 32 was a photograph from the actual testing, just after a sample had a transverse failure during the test run.

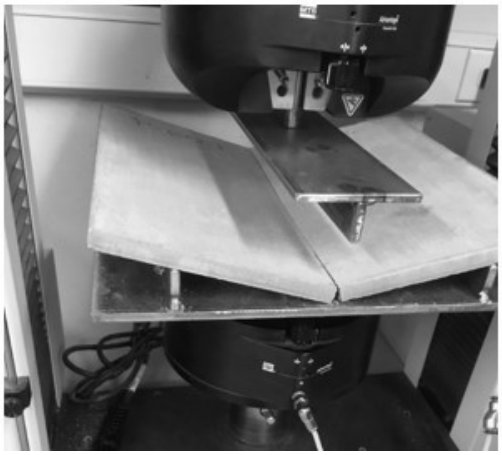

Figure 32. Photograph of a Biochar-Gypsum Sample in the MTS Insight 5 Testing System, just after Transverse Failure during the Flexural Strength Test

CHAPTER 4

STATISTICAL ANALYSES AND RESULTS

Summary of the Statistical Tests

In this section, the data gathered from the thermal conductivity and flexural strength tests, as well as the measurements of density, were provided. The P.100 control group, and the P.90 – P50A experimental groups were used to test the null hypotheses, that there was no difference between the group means of these attributes. The tests, secondarily, looked at the trends that occurred as higher percentages of biochar were added to the experimental mixtures in the P.90 - P.50A groups.

The statistical tests that were run include first, the Shapiro-Wilk test for normality of data. Next, Levene's Test for homogeneity of variances between the sample groups was conducted. The thermal conductivity and the flexural strength test results were that the sample groups did not have similar variances, so a standard ANOVA, comparing group means, would not produce valid results. Instead, a Brown-Forsythe test was conducted, which determined that differences in group means existed among the groups. Then, a post-hoc Games-Howell test was conducted that showed which sample groups possessed different means of thermal conductivity and flexural strength tested. For the density test results, an ANOVA, then a post-hoc Tukey's HSD test, was conducted to determine which sample groups possessed different means of density.

Power of the Study Calculation

In general, the power of a study is defined as "the probability of rejecting the null hypothesis when the alternative hypothesis is true" (McCrum-Gardner, 2010, p. 11). The

minimum accepted level of the power of a study is considered by many sources as 80%, first given by Cohen (1988), and used and verified by others (Ellis, 2006; McCrum-Gardner, 2010; Skrivanek, 2009).

McCrum-Gardner (2010) provided information on software packages that can be used to calculate the power of the study. Of the four software packages mentioned in the journal article, only two were still available for use, Minitab and PS software.

Minitab (2016) has the ability to calculate power and sample size, before an experiment is performed, a prospective study, or after an experiment is performed, a retrospective study.

A prospective study means that power is calculated before the test was conducted. A calculation of the power, using data like means and variances of sample groups gathered by research from past studies, will help the researcher be able to detect differences (effects) that are considered important. It allows the researcher the opportunity to increase design sensitivity, by increasing the sample size or by taking measures to decrease the error variance. A retrospective study, done after data is gathered, is more appropriate when there is no past research that provides estimates of means or variances of groups. A retrospective study can still help the researcher understand the power of the tests that have already been performed (Minitab, 2016).

For this study, the power of the test was not calculated before this study was conducted, because no previous research on the topic of finding the effects on thermal conductivity of a biochar-gypsum composite was found. No estimations of means or variances for biochar-gypsum mixes were available to use as a basis for determining

sample sizes, prior to testing. Thus, only a retrospective study of the data was pursued to calculate the power of the study, as follows.

It was decided that the power of the study calculations would be made with the P.100 and P.90 sample group's data only, to assure that the smallest possible difference in group means, between the control and experimental groups, was being tested.

The input variables entered into Minitab to calculate a value for power were:

Level for α, the Type I error probability for a two sided test, was chosen as $\alpha = 0.05$.

Number of levels: For this study, considering only the P.100 control group and the P.90 experimental group, the number of levels = 2.

Sample sizes: For this study, there were 5 samples in each group.

Values of the maximum difference between means: This value comes from the data gathered by the thermal conductivity testing. From Table 17, the researcher used the difference of mean values for the P.100 and P.90 groups = 0.3437 – 0.3137 = 0.0300.

Power value: This was the value calculated by the retrospective power test.

Standard deviation: This value comes from the data gathered by the thermal conductivity testing. From Table 17, the researcher used the calculated standard deviation = 0.01279 of the P.100 sample group, the larger of the standard deviations from the P.100 control group and the P.90 experimental group.

These data were input into the proper test in Minitab, and a Power = 0.899435 value was calculated, as seen in Table 15.

Table 15

Minitab Results for Power Calculation

α = 0.05	Assumed standard deviation = 0.01279	
Factors: 1	Number of levels: 2	
Maximum Difference	Sample Size	Power
0.0300	5	0.899435

Minitab also produced a Power Curve graph, as seen in Figure 33, that gives a visual representation of the power calculation versus the maximum difference of means from the tests.

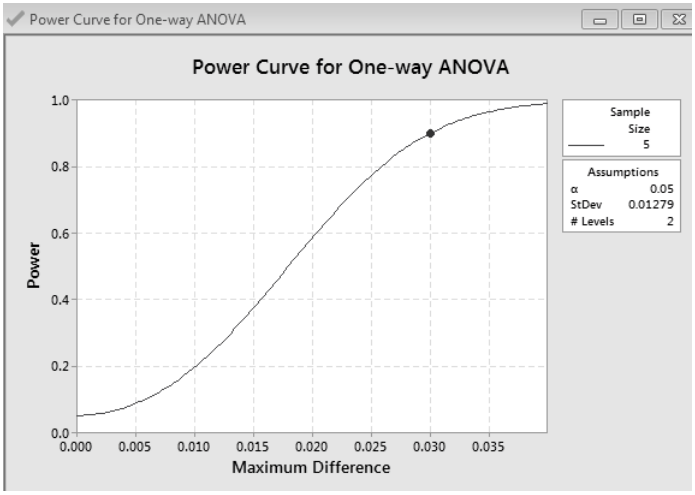

Figure 33. Power Curve using P.100 and P.90 Sample Groups Only

As a check on the validity of the Minitab power test, a second software was also used to calculate a value for power. This was the Power and Sample Size (PS) Calculator (Department of Biostatistics, Vanderbilt University, 2013). In the PS software, the

alternative hypothesis can be specified either in terms of differing means, survival times, or regression slopes or intercepts. Studies may involve either a matched or independent study designs (Department of Biostatistics, Vanderbilt University, 2013).

This study was looking at the difference between group means and used independent measurements of each group of samples. According to the Department of Biostatistics, Vanderbilt University (2013), there are eight different types of study designs that can be evaluated using PS software. This study fits their definition of design number eight, continuous response measures in two groups - paired and independent t-tests.

The PS software defined these input variables needed to run the power calculation:

α = The Type I error probability for a two sided test. This is the probability that we will falsely reject the null hypothesis. For all of this study, a level of significance of 0.05 was chosen.

n = For independent t-tests, n is the number of experimental subjects. For this study there were 5 samples in each group.

Power = This was the value calculated by the test.

δ = A difference in population means. This value comes from the data gathered by the thermal conductivity testing. From Table 17, the researcher used the difference of group means between the P.100 and P.90 groups, $\delta = 0.3437 - 0.3137 = 0.0300$.

σ = For independent tests, σ is the within group standard deviation. This value comes from the data gathered by the thermal conductivity testing. From Table 17, the

researcher used σ = 0.01279, the larger of the standard deviations from the P.100 and P.90 sample groups.

m = For independent tests m is the ratio of control to experimental patients. For this test, m = 1.

The results of running PS software with these inputs are shown in Figure 34. The PS software calculated that Power = 0.901.

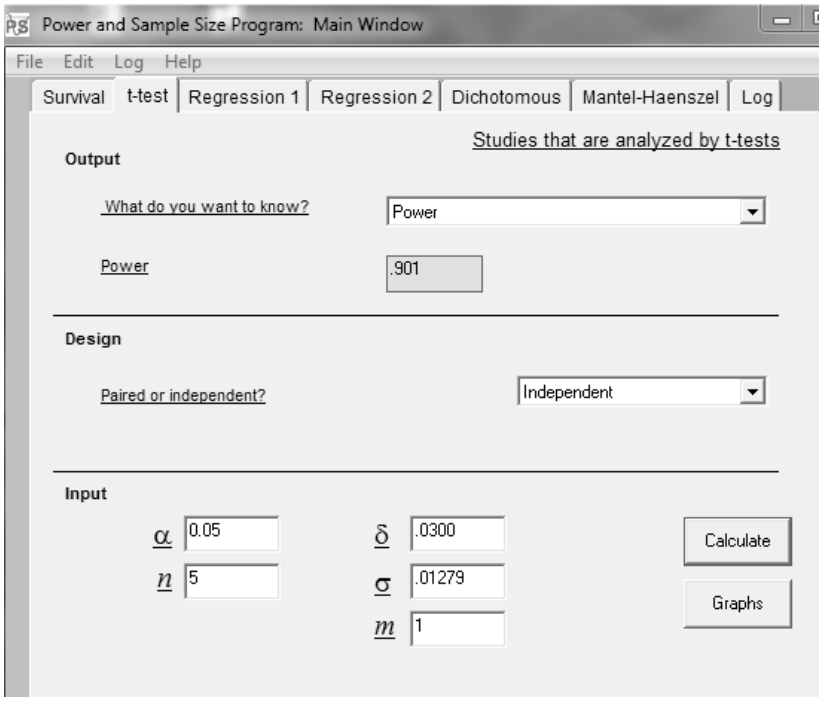

Figure 34. PS Software Analysis Input Data and Results, using P.100 and P.90 Sample Groups Only

After the PS software ran, it also produced this description, in terms of a prospective study, about what was calculated.

> We are planning a study with 5 experimental subjects and 5 control subjects. In a previous study the response within each subject group was normally distributed with standard deviation 0.01279. If the true difference in the experimental and

> control means is 0.0300, we will be able to reject the null hypothesis that the population means of the experimental and control groups are equal with probability (power) 0.901. The Type I error probability associated with this test of this null hypothesis is 0.05 (Department of Biostatistics, Vanderbilt University, 2013).

These results would be equally valid for a restrospective study, changing the wording to “current study found the standard deviation 0.01279”, “measured difference . means is 0.3000” and “we are able to reject the null hypothesis … power 0.901”.

According to Ellis, there is nothing “cast in stone regarding the appropriate level of statistical power” (2006, p. 1), but it is generally accepted that studies should have an 80% probability of detecting an effect, when an effect exists that can be detected. This value of 80% means that there is a 20% probability of not rejecting the null hypothesis when the alternative hypothesis is true, a Type II error.

Two independent software calculations of power, Minitab and PS, using a retrospective study approach, produced very similar results from the data gathered by testing the thermal conductivity of the P.100 and P.90 samples. Using only those sample groups, with the data gathered using five samples for each group, both tests produced a power > 80%, as seen in Table 16.

Table 16

Summary of Calculations of Power of the Study

Software Used	Power Calculated
PS	0.901
Minitab	0.899435

The conclusion was that the choice of producing five samples to be tested, from both the P.100 control group and the P.90 – P.50A experimental groups, produced results that were statistically significant, and conclusions could be made about the results found.

Statistical Tests Used in this Study

Statistical tests were run in order to test these hypotheses:

$H_0$1: There is no difference between the thermal conductivity of biochar-gypsum mix and the thermal conductivity of gypsum alone.

Ha1: There is a statistically significant difference between the thermal conductivity of biochar-gypsum mix and the thermal conductivity of gypsum alone.

The other two hypotheses were similar, checking for differences between the control and experimental groups for density and flexural strength.

The standard statistical test for difference of means between two groups is a paired-t test. In order to run this test the dependent variables must be normally distributed, the groups must be independent, and the variance of each group must be equal (Laerd Statistics, 2013a). When there are more than two groups to compare, then the one-way analysis of variance (ANOVA) is used. Just as with the paired t-test, the dependent variables must be normally distributed, the groups must be independent, and the variance of each group must be equal (Laerd Statistics, 2013b). Looking at the data set being tested, one other characteristic that must be considered to determine the appropriate statistical test to run was that there was a small sample size for each group.

First a Shapiro-Wilk test was conducted. “The SPSS Shapiro-Wilk Test was more appropriate than the Kolmogorov-Smirnov test for small sample sizes (< 50 samples)”

(Laerd Statistics, 2013c, p. 5). A Shapiro-Wilk test was used to calculate a p-value for testing the null hypothesis that the data follow a normal distribution, versus the alternative hypothesis that the data do not follow a normal distribution. Choosing a confidence interval of 0.95, if the Shapiro-Wilk test returns a p value > 0.05, then the decision is to fail to reject the null hypothesis, and conclude that the data do follow a normal distribution (Laerd Statistics, 2013c).

Next, a Levene's Test was conducted to see if the sample groups had similar variances. For the thermal conductivity and flexural strength data, the group variances were not equal. For the density test data, the group variances were equal.

If the data were normally distributed, a Brown-Forsythe test, which can be used when using groups with non-homogeneous variances, was conducted to test if there are differences in group means. The Brown-Forsythe test "uses a different denominator for the formula of F in the ANOVA. Instead of dividing by the mean square of the error, the mean square is adjusted using the observed variances of each group." (XLStat, 2015, p. 1). In this test, if the value returned was within the test limit of $p < 0.05$, then difference in group means existed in the data.

Lastly, to find where the specific group differences were, a post-hoc Games-Howell test was conducted. The Games-Howell test can be used when group variances are not equal (as in the case of this study data) and also takes into account unequal group sizes (not the case in this study). "This test appears to do better than the Tukey HSD if variances are very unequal (or moderately so in combination with small sample size) or can be used if the sample size per cell is very small (e.g., < 6)" (Newsom, 2006, p. 3).

Both of these conditions were true for the thermal conductivity and flexural strength data in this study.

For the density test data, which did have homogeneous variances among the sample groups, a standard ANOVA was conducted to determine if there were differences in group means, and then a post-hoc Tukey's HSD (Honestly Significant Difference) test was conducted. The Tukey distribution gives "the exact sampling distribution of the largest difference between a set of means originating from the same population. All pairwise differences are evaluated using the same sampling distribution used for the largest difference" (Abdi & Williams, 2010, p. 1).

As a final step, to help in visualizing the group means differences, a SPSS Means Plot was conducted on all three sets of data.

Thermal Conductivity Data and Statistical Analysis

Table 17 gives the thermal conductivity, k, in units of W/(m-Kelvin), values measured for the control group and each of the experimental groups' samples, along with each group's mean and standard deviation.

Table 17

Thermal Conductivity Test Data and Calculated Group Means and Standard Deviations

Sample	k (W/m-Kelvin)	Group Mean	Group Std. Dev.
P.100.1	0.3289		
P.100.2	0.3470		
P.100.3	0.3473	0.3437	0.01279
P.100.4	0.3339		
P.100.5	0.3615		
P.90.1	0.3057		
P.90.2	0.3253		
P.90.3	0.3134	0.3137	0.00972
P.90.4	0.3028		
P.90.5	0.3215		
P.80.1	0.2941		
P.80.2	0.3061		
P.80.3	0.3081	0.3003	0.00772
P.80.4	0.3028		
P.80.5	0.2904		
P.70.1	0.3069		
P.70.2	0.2986		
P.70.3	0.2927	0.2988	0.00757
P.70.4	0.2901		
P.70.5	0.3059		
P.60.1	0.2775		
P.60.2	0.2712		
P.60.3	0.2930	0.2858	0.01122
P.60.4	0.2986		
P.60.5	0.2887		
P.50.1A	0.2669		
P.50.2A	0.2483		
P.50.3A	0.2900	0.2701	0.01494
P.50.4A	0.2729		
P.50.5A	0.2724		

First, the data was checked to see if it was normal in distribution. As seen in Table 18, for the control group P.100, and all five of the experimental groups, P.90 through P.50A, the SPSS Shapiro-Wilk test returned a significance of 0.408 or higher, suggesting that the data collected for each group could be considered normally distributed.

Table 18

Shapiro-Wilk Test for Normality of the Thermal Conductivity Test Data

Percent Plaster	Shapiro-Wilk		
	Statistic	df	Sig.
50	0.951	5	0.742
60	0.952	5	0.752
70	0.900	5	0.408
80	0.906	5	0.445
90	0.931	5	0.604
100	0.946	5	0.706

The normality information can be seen graphically using the SPSS Q-Q Normality plots, shown in Figure 35. In these plots, data points should be evenly distributed above and below the line present, if the data collected was normally distributed (Laerd Statistics, 2013c). In these graphs, the data points do appear evenly distributed.

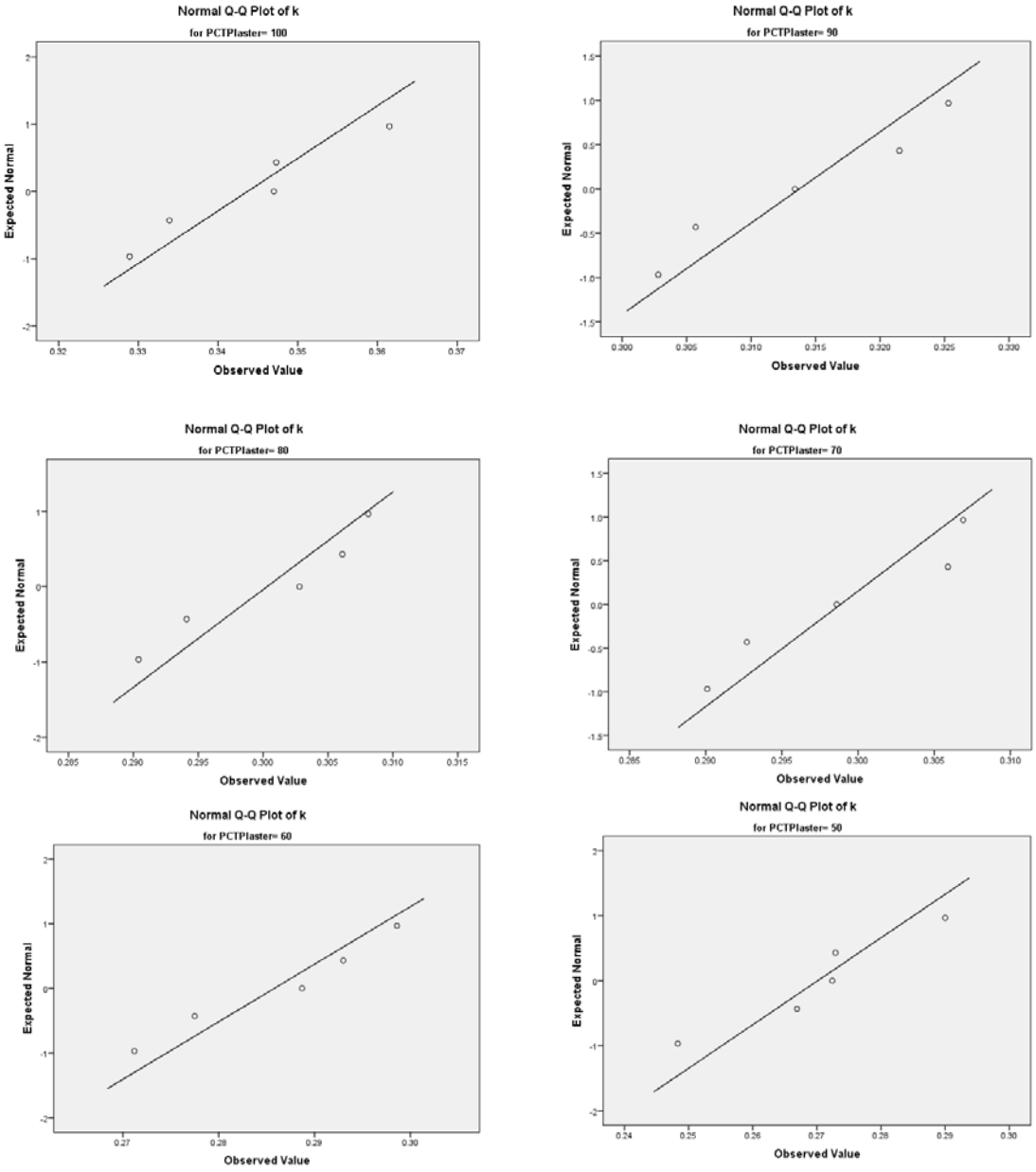

Figure 35. Q-Q Normality Plots for the Various Mixtures of Biochar-Gypsum from the Thermal Conductivity Test Data

Next, an SPSS Levene's Test was conducted, to test the sample groups for homogeneity of variances. Table 19 shows the results of that test, with the Levene

statistic = 0.442, with a significance = 0.815, suggesting that the variances of the sample groups were not homogeneous.

Table 19

Test of Homogeneity of Variances for Thermal Conductivity Data

Thermal conductivity, k			
Levene Statistic	df1	df2	Sig.
0.442	5	24	0.815

Next, a Brown-Forsythe tests was conducted, as seen in Table 20. The results of this test suggested, with a value of $p < 0.0001$, well within the $p < 0.05$ limit chosen by this study, that differences of means between groups existed in the data. However, this test did not reveal where the differences were.

Table 20

Brown-Forsythe Test Results of the Thermal Conductivity Test Data

Thermal conductivity, k				
	Statistic[a]	df1	df2	Sig.
Brown-Forsythe	26.236	5	19.365	0.000

a. Asymptotically F distributed.

To find out where the difference in group means were, a post-hoc SPSS Games-Howell test was conducted. Table 21 shows the results of this test. Statistically significant differences of group means were marked by a '*'.

Table 21

Games-Howell Post-Hoc Test of Thermal Conductivity Test Data

Sample Group	Compared to Group	Mean Difference	Sig.	95% Confidence Interval	
				Lower Bound	Upper Bound
50	60	-0.0157000	0.479	-0.046883	0.015483
	70	-0.0287400	0.059	-0.058707	0.001227
	80	-.0302000*	0.048	-0.060171	-0.000229
	90	-.0436400*	0.008	-0.074040	-0.013240
	100	-.0736200*	0.000	-0.105984	-0.041256
60	50	0.0157000	0.479	-0.015483	0.046883
	70	-0.0130400	0.360	-0.036010	0.009930
	80	-0.0145000	0.277	-0.037531	0.008531
	90	-.0279400*	0.025	-0.052367	-0.003513
	100	-.0579200*	0.001	-0.085887	-0.029953
70	50	0.0287400	0.059	-0.001227	0.058707
	60	0.0130400	0.360	-0.009930	0.036010
	80	-0.0014600	1.000	-0.019100	0.016180
	90	-0.0149000	0.182	-0.035345	0.005545
	100	-.0448800*	0.003	-0.070672	-0.019088
80	50	.0302000*	0.048	0.000229	0.060171
	60	0.0145000	0.277	-0.008531	0.037531
	70	0.0014600	1.000	-0.016180	0.019100
	90	-0.0134400	0.257	-0.033982	0.007102
	100	-.0434200*	0.004	-0.069245	-0.017595
90	50	.0436400*	0.008	0.013240	0.074040
	60	.0279400*	0.025	0.003513	0.052367
	70	0.0149000	0.182	-0.005545	0.035345
	80	0.0134400	0.257	-0.007102	0.033982
	100	-.0299800*	0.029	-0.056739	-0.003221
100	50	.0736200*	0.000	0.041256	0.105984
	60	.0579200*	0.001	0.029953	0.085887
	70	.0448800*	0.003	0.019088	0.070672
	80	.0434200*	0.004	0.017595	0.069245
	90	.0299800*	0.029	0.003221	0.056739

* = The mean difference is significant at the 0.05 level.

These results suggested that the experimental study of thermal conductivity showed there was a statistically significant difference, with $p < 0.05$, between the mean of the control group, P.100, and the means of the experimental groups P.90 – P.50A. Therefore, the null hypothesis $H_0 1$ was rejected in favor of the alternative hypothesis Ha1, and the conclusion was made that adding biochar to gypsum decreased the thermal conductivity of the resulting mix. In more generic terms, the thermal insulation value increased.

The results further suggested that thermal conductivity decreased as the percentage of biochar was increased, but not necessarily in a statistically significant manner for each 10% increase in biochar content.

A graphical representation of these differences in means can be seen more clearly using the SPSS Means Plot function, as seen in Figure 36. This plot showed the 95% confidence interval of the mean, of the control and experimental groups.

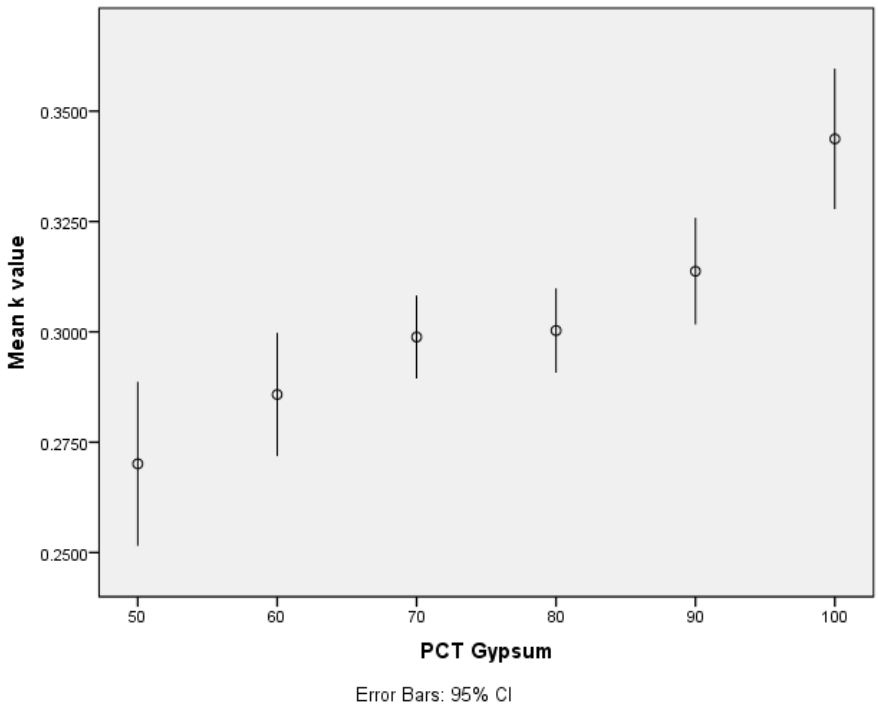

Figure 36. Group Means Plot of Thermal Conductivity vs. Percent Gypsum

Data and Statistical Analysis on Density

Table 22 shows the density calculated for the control group and each of the experimental groups' samples, along with each group's mean and standard deviation.

Table 22

Density Test Data and Calculated Group Means and Standard Deviations

Sample	Density (g / cm^3)	Group Mean	Group Std. dev.
P.100.1	1.239		
P.100.2	1.235		
P.100.3	1.239	1.2394	0.01305
P.100.4	1.26		
P.100.5	1.224		
P.90.1	1.219		
P.90.2	1.199		
P.90.3	1.111	1.156	0.05697
P.90.4	1.085		
P.90.5	1.166		
P.80.1	1.031		
P.80.2	1.092		
P.80.3	1.073	1.0464	0.03406
P.80.4	1.017		
P.80.5	1.019		
P.70.1	1.143		
P.70.2	0.987		
P.70.3	0.985	1.0562	0.06942
P.70.4	1.098		
P.70.5	1.068		
P.60.1	1.045		
P.60.2	1.006		
P.60.3	0.988	1.0316	0.03278
P.60.4	1.058		
P.60.5	1.061		
P.50.1A	0.913		
P.50.2A	0.901		
P.50.3A	0.851	0.9082	0.03695
P.50.4A	0.925		
P.50.5A	0.951		

First, the data was checked to see if it was normally distributed. The SPSS Shapiro-Wilk Test, as seen in Table 23, returned a significance of 0.202 or higher for all

groups, suggesting that the density data collected for each group can be considered normally distributed.

Table 23

Shapiro-Wilk Test for Density Data

Percent Plaster	Shapiro-Wilk		
	Statistic	df	Sig.
50	0.956	5	0.781
60	0.868	5	0.258
70	0.901	5	0.416
80	0.852	5	0.202
90	0.937	5	0.645
100	0.910	5	0.465

Next, an SPSS Levene's Test was conducted, to test the sample groups for homogeneity of variances. Table 24 shows the results of that test, with the Levene statistic = 3.733, with a significance = 0.012, suggesting that the variances of the sample groups for density were homogeneous.

Table 24

Test of Homogeneity of Variances of Density Data

Density			
Levene Statistic	df1	df2	Sig.
3.733	5	24	0.012

With data groups that do have homogeneity of variances, the test to see if means differ is a One-way ANOVA. Table 25 shows the results of the ANOVA for the density data. The results of this test suggested, with a value of $p < 0.0001$, well within the $p < 0.05$ limit chosen by this study, that there existed in the data differences of means between groups. However, this test did not reveal where the differences were.

Table 25

ANOVA for Density Data

	Sum of Squares	df	Mean Square	F	Sig.
Between Groups	0.322	5	0.064	32.669	0.000
Within Groups	0.047	24	0.002		
Total	0.370	29			

To find out where the difference in group means was, an SPSS post-hoc Tukey HSD test was conducted. Table 26 shows the results of this test. Statistically significant differences of group means were marked by a '*'.

There was not a statistically significant difference, between the means of density of the control P.100 group and the experimental P.90 group. There were differences between the mean of the control group, P.100, and the means of all the other experimental groups, P.80 to P.50A.

Table 26

Post-Hoc Tukey HSD Test of Density Test Data

Sample Group	Compared to Group	Mean Difference	Sig.	95% Confidence Interval	
				Lower Bound	Upper Bound
50	60	-.123400*	0.002	-0.21025	-0.03655
	70	-.148000*	0.000	-0.23485	-0.06115
	80	-.138200*	0.001	-0.22505	-0.05135
	90	-.247800*	0.000	-0.33465	-0.16095
	100	-.331200*	0.000	-0.41805	-0.24435
60	50	.123400*	0.002	0.03655	0.21025
	70	-0.024600	0.949	-0.11145	0.06225
	80	-0.014800	0.995	-0.10165	0.07205
	90	-.124400*	0.002	-0.21125	-0.03755
	100	-.207800*	0.000	-0.29465	-0.12095
70	50	.148000*	0.000	0.06115	0.23485
	60	0.024600	0.949	-0.06225	0.11145
	80	0.009800	0.999	-0.07705	0.09665
	90	-.099800*	0.018	-0.18665	-0.01295
	100	-.183200*	0.000	-0.27005	-0.09635
80	50	.138200*	0.001	0.05135	0.22505
	60	0.014800	0.995	-0.07205	0.10165
	70	-0.009800	0.999	-0.09665	0.07705
	90	-.109600*	0.008	-0.19645	-0.02275
	100	-.193000*	0.000	-0.27985	-0.10615
90	50	.247800*	0.000	0.16095	0.33465
	60	.124400*	0.002	0.03755	0.21125
	70	.099800*	0.018	0.01295	0.18665
	80	.109600*	0.008	0.02275	0.19645
	100	-0.083400	0.065	-0.17025	0.00345
100	50	.331200*	0.000	0.24435	0.41805
	60	.207800*	0.000	0.12095	0.29465
	70	.183200*	0.000	0.09635	0.27005
	80	.193000*	0.000	0.10615	0.27985
	90	0.083400	0.065	-0.00345	0.17025

* = The mean difference is significant at the 0.05 level.

These results suggested that the experimental study produced data about density that showed there was a statistically significant difference, with $p < 0.05$, between the

mean of the control group, P.100, and the means of the experimental groups P.90 – P.50A. Therefore, the null hypothesis $H_0$2 was rejected in favor of the alternative hypothesis Ha2, and the conclusion was made that adding biochar to gypsum decreased the density of the resulting mix.

The results further suggested that density decreased as the percentage of biochar was increased, but not necessarily in a statistically significant manner for each 10% increase in biochar content.

A graphical representation of these differences in means can be seen more clearly using the SSPS Means Plot function, as seen in Figure 37. This plot shows the 95% confidence interval of the group means for density.

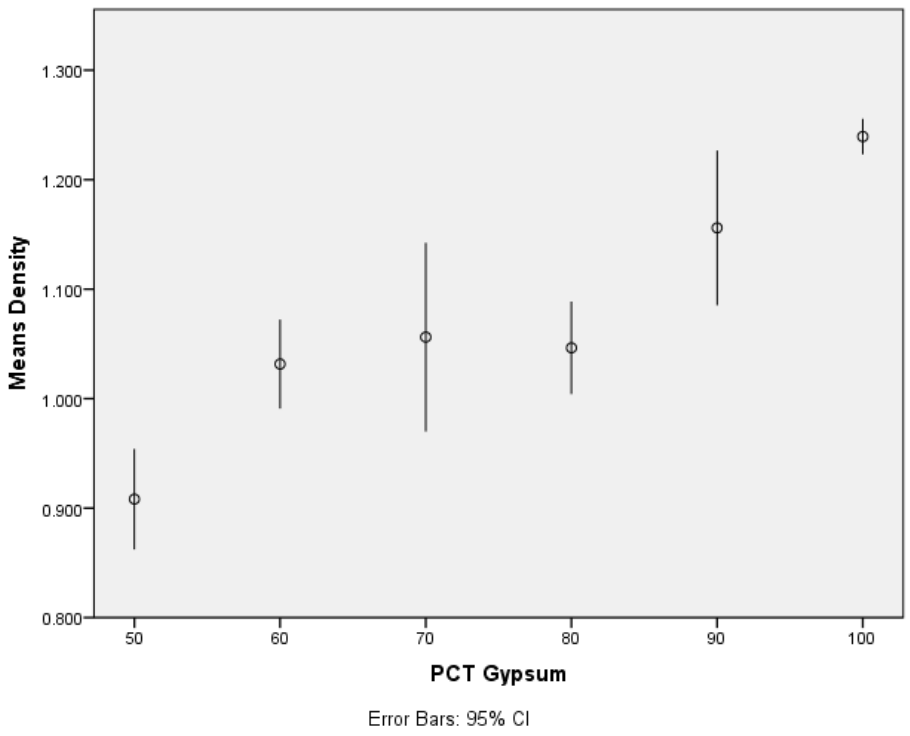

Figure 37. Group Means Plot for Density Data

Data and Statistical Analysis on Flexural Strength

Table 27 gave the flexural strength measured for the control group and each of the experimental groups' samples, along with each group's mean and standard deviation.

Table 27

Flexural Strength Test Data and Calculated Group Means and Standard Deviations

Sample	Flexural Strength (Newtons at breaking point)	Group Mean	Group Std. dev.
P.100.1	651.33		
P.100.2	619.58		
P.100.3	470.03	570.99	74.49
P.100.4	519.61		
P.100.5	594.4		
P.90.1	481.75		
P.90.2	566.08		
P.90.3	263.65	457.01	127.46
P.90.4	405.19		
P.90.5	568.39		
P.80.1	142.41		
P.80.2	408.06		
P.80.3	229.50	250.67	101.36
P.80.4	280.03		
P.80.5	193.32		
P.70.1	404.03		
P.70.2	228.02		
P.70.3	302.53	312.86	66.95
P.70.4	348.79		
P.70.5	280.93		
P.60.1	201.38		
P.60.2	223.62		
P.60.3	184.86	246.11	77.17
P.60.4	242.15		
P.60.5	378.57		
P.50.1A	169.81		
P.50.2A	88.10		
P.50.3A	86.29	144.58	53.59
P.50.4A	200.58		
P.50.5A	178.15		

First, the data was checked to see if it was normally distributed. The SPSS Shapiro-Wilk Test, as seen in Table 28, returns a significance of 0.141, or higher, for the P.100, P.90, P.80, P.70, and P.50A groups, but only p = 0.091 for the P.60 group. This result for the Shapiro-Wilk test was technically above the p > 0.05 level, but so close to it that the decision by the researcher was to conclude that the P.60 group data was not normally distributed.

Table 28

Shapiro-Wilk Test for Normality of the Flexural Strength Test Data

Percent	Shapiro-Wilk		
Plaster	Statistic	df	Sig.
50	0.831	5	0.141
60	0.806	5	0.091
70	0.992	5	0.987
80	0.949	5	0.731
90	0.897	5	0.391
100	0.942	5	0.683

Looking at the data for the P.60 group, the P.60.5 sample had a flexural strength of 378 N., which was far away from the average of the other four P.60 samples, 213 N. This led to the decision that the P.60.5 sample should be treated as an outlier that should be discarded from the group. Since the sample size of 5 per group was so small, this led to the decision that the entire P.60 group should be discarded from the flexural strength analysis. With the P.60 group removed from the data, the Shapiro-Wilk statistic on the

remaining groups suggested that the data in the groups were normally distributed. As the data to be analyzed for flexural strength was changed, a descriptive statistics table (Table 29) was generated, rather than repeating a reduced Table 27.

Table 29

Descriptive Statistics for Flexural Strength Data with the P.60 Sample Group Removed

PCT Plaster	N	Mean	Std. Deviation	95% Confidence Interval of Mean	
				Lower Bound	Upper Bound
50	5	144.6	53.6	78.04	211.12
70	5	312.9	66.9	229.7	395.99
80	5	250.7	101.4	124.81	376.51
90	5	457.0	127.5	298.74	615.28
100	5	571.0	74.5	478.49	663.48

Next, an SPSS Levene's Test was conducted, to test the sample groups for homogeneity of variances. Table 30 shows the results of that test, with the Levene statistic = 1.11, with a significance = 0.379, suggesting that the variances of the sample groups were not homogeneous.

Table 30

Test of Homogeneity of Variances of Flexural Strength Test Data

Flexural Strength			
Levene Statistic	df1	df2	Sig.
1.111	4	20	0.379

Next, a Brown-Forsythe tests was conducted, as seen in Table 31. The results of this test suggested, with a value of $p < 0.0001$, well within the $p < 0.05$ limit chosen by this study, that there existed in the data differences of means between groups. However, this test did not reveal where the differences were.

Table 31

Brown-Forsythe Test Results of the Flexural Strength Test Data

Flexural Strength				
	Statistic[a]	df1	df2	Sig.
Brown-Forsythe	18.025	4	14.504	0.000
a. Asymptotically F distributed.				

To find out where the difference in means was, a post-hoc SPSS Games-Howell test was conducted, as shown in Table 32, with $p < 0.05$ differences of group means marked with a '*'. There was not a difference in flexural strength between the P.100 control group and experimental P.90 group, but there was a difference between the P.100 control group and the remaining experimental groups, P.80, P.70, and P.50A.

These results suggested that the experimental study produced data about flexural strength that showed there was a statistically significant difference, with $p < 0.05$, between the mean of the control group, P.100, and the means of the experimental groups P.90 – P.50A. Therefore, the null hypothesis $H_0 3$ was rejected in favor of the alternative

hypothesis Ha3, and the conclusion was made that adding biochar to gypsum decreased the flexural strength of the resulting mix.

The results further suggested that flexural strength decreased as the percentage of biochar was increased, but not necessarily in a statistically significant manner for each 10% increase in biochar content.

Table 32

Games-Howell Post-Hoc Test for the Flexural Strength Test Data with P.60 Group Removed

Sample Group	Compared to Group	Mean Difference	Sig.	95% Confidence Interval	
				Lower Bound	Upper Bound
50	70	-168.27760*	0.016	-302.33	-34.22
	80	-106.08	0.338	-297.63	85.47
	90	-312.42780*	0.017	-553.64	-71.21
	100	-426.40840*	0	-571.74	-281.07
70	50	168.27760*	0.016	34.22	302.33
	80	62.19	0.78	-132.71	257.10
	90	-144.15	0.28	-385.00	96.70
	100	-258.13080*	0.003	-413.30	-102.96
80	50	106.08	0.338	-85.47	297.63
	70	-62.19	0.78	-257.10	132.71
	90	-206.34	0.121	-461.09	48.40
	100	-320.32500*	0.004	-518.95	-121.70
90	50	312.42780*	0.017	71.21	553.64
	70	144.15	0.28	-96.70	385.00
	80	206.34	0.121	-48.40	461.09
	100	-113.98	0.48	-356.01	128.05
100	50	426.40840*	0	281.07	571.74
	70	258.13080*	0.003	102.96	413.30
	80	320.32500*	0.004	121.70	518.95
	90	113.98	0.48	-128.05	356.01

* = The mean difference is significant at the 0.05 level.

A graphical representation of these differences in means can be seen more clearly using the SSPS Means Plot function, as seen in Figure 38. This plot shows the 95% confidence interval of the group means.

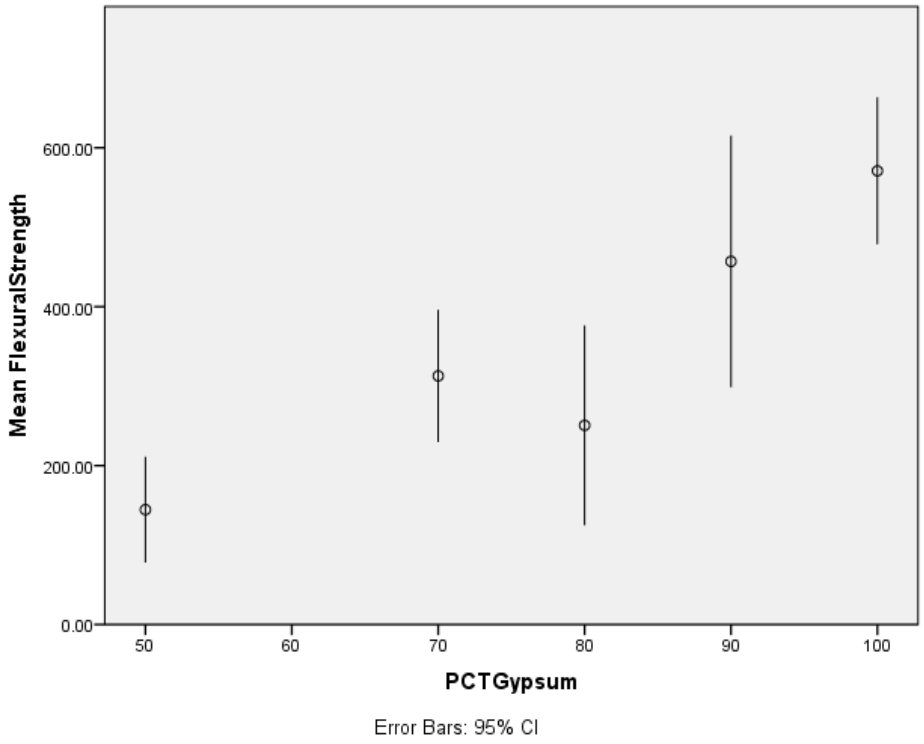

Figure 38. Group Means Plot for the Flexural Strength Test, with the P.60 Sample Group Removed

Thermal Conductivity of Biochar

The thermal conductivity of the biochar was found, for example using the numbers from Biochar sample #1, and using equation (28) determined in the Chapter 3 Methodology section,

$$\text{Rbiochar} = \text{Rpanel} - \text{Rglass} = 0.08565 - 0.00496 = 0.08069 \ \frac{\text{m}^2 * \text{Kelvin}}{\text{W}} \qquad (30)$$

Converting to thermal conductivity of the biochar sample alone:

$$k = \frac{\text{thickness}}{\text{Rbiochar}} = \frac{0.0127\ \text{m}}{0.08069\ \frac{\text{m}^2 * \text{Kelvin}}{\text{W}}} = 0.1573 \frac{\text{W}}{\text{m} * \text{Kelvin}} \quad (31)$$

The glass-biochar panel was filled with loose biochar four more times, a test was conducted, and a k value was calculated each time, producing the results seen in Table 33. This test produced a value of thermal conductivity for biochar that was less than any of the experimental biochar-gypsum samples measured. These values can only be used as a reference, as biochar alone, or a biochar-glass panel, cannot be used as a structural or insulating material as a replacement for gypsum board.

Table 33

Thermal Conductivity Test Data of Bulk Biochar and Calculated Group Means and Standard Deviations

Sample	k (W/m-Kelvin)	Group Mean	Group Std. Dev.
Biochar #1	0.1573		
Biochar #2	0.1863		
Biochar #3	0.1779	0.1733	0.0157
Biochar #4	0.1888		
Biochar #5	0.1560		

CHAPTER 5

CONCLUSIONS AND RECOMMENDATIONS

This study was an initial step in a series of projects to test the possibility of improving thermal performance of gypsum board by inclusion of biochar and creating a bio-based composite for construction. The goal of this research was to study the effect of corn stover biochar's inclusion on thermal conductivity, flexural strength and density of the composite. The research was unique as it compared the potential adverse effect on flexural strength along with the improved thermal performance to provide the base for future research of the composite. Additionally, the researcher measured the thermal conductivity of corn stover biochar to set the base of further investigation in the area.

The results of this research filled in the gap in empirical studies on improving the thermal performance of gypsum board by inclusion of biochar. The results from the flexural strength of the composite proved that including biochar within certain range in gypsum board could produce a product meeting and in some cases exceeding the current ASTM C1396 (ASTM International, 2014g) standards for ½ inch gypsum board.

Due to time and funding constraints the process of making the samples for this study varies from the commercially available gypsum board. The typical process for manufacturing gypsum board entails adding foam to the slurry of gypsum and water in the mixer to make it lightweight, thus impacting the properties of the gypsum board. In a different processing step, the gypsum slurry is poured between two layers of paper or fiberglass mats, which affects the flexural strength and thermal conductivity of the product. The drying process in a manufacturing facility is completed in a kiln leaving the

gypsum board literally moisture–free. Through the manufacturing process, the product quality of gypsum board is ensured by computerized process control systems, and frequently tested in lab (Georgia-Pacific, 2016). Typical manufacturing process also entails additives different from gypsum and water in the slurry to enhance certain properties of the product, such as strength and fire resistance (Allen & Iano, 2014).

This research focused on studying the effect of biochar when mixed with gypsum and water only to serve as base for further studies. To produce valid empirical results it was necessary to eliminate the effect of foaming, or property altering additives.

Conclusions

Thermal Conductivity

Based on the results from the thermal conductivity tests, the researcher found that including biochar in gypsum decreased the thermal conductivity of the composite. The incremental increase of biochar led to an incremental decrease of thermal conductivity. Additionally, the results from the experimental groups were not consistent with the rate of change of biochar. This may be the result of error due to fact that the researcher used a hand–held drill for mixing, leading to inconsistency of the blend, or due to error in measurement procedure.

Density

The calculations on density suggested that that inclusion of biochar led to decrease of density. The researcher expected that tests results for density would follow exactly the pattern of changes in thermal conductivity among the experimental groups. However, the change in density among experimental groups did not follow the pattern of

changes in thermal conductivity. This surprising finding could be the result of minor deformation of wood molds, causing deviations from the thickness of the samples from the designed 1/2 inch.

Flexural Strength

The results from the flexural strength tests also led to rejection of the null hypothesis. The P.90 experimental group showed an unusually wide range of standard deviation from the mean, which when compared to the control group did not show a statistically significant difference. This was not observed in any of the other four experimental groups. The researcher could not explain this abnormality for the P.90 experimental group, especially when compared to results from thermal conductivity tests. Further investigations with a larger sample size are necessary to check if this behavior could be due to some unusual chemistry between biochar and gypsum, or due to variations in the homogeneity of the mix.

The test results also indicated that within certain range of proportions for the design, the samples featured flexural strength well within the range specified by ASTM C 1396 standard, which makes this research valuable for further investigations. The results of this research are valuable for the construction industry as new bio-based component can become reality.

The study added new knowledge in the efforts to improve thermal performance of gypsum board conducted by others in the past. It also set the grounds for reducing the need of the manufacturing industries for non-renewable natural material, gypsum, by substitution with biochar.

Recommendations for Research Design and Methodology

Sample Size

The time constraints for this study dictated small sample size. Larger sample size is highly recommended to reduce the risk of inconsistent patterns (varying differences between groups' standard deviations). Smaller incremental change, 5% for example, of biochar to gypsum proportions in the experimental groups, is suggested for further investigation of the effect of biochar on the properties of the mixture.

Materials

Different ranges of size of corn stover biochar are recommended to explore the effect of size on thermal conductivity, density, and flexural strength of biochar-gypsum, so that the effect of size of biochar properties under investigation could be compared.

Similar research should be carried out with different types of biochar and gypsum, as the origin of biochar could be a major factor on the thermal conductivity, density, and flexural strength of the composite.

Mold Material

Due to limitations of funding this research used wood for creating the molds. The tendency of wood to deform due to variation of humidity and contact with moisture caused minor variations in thicknesses of samples. Stainless steel, or a plastic with sufficient stiffness, molds will produce uniform dimension of the samples. Leveling of the support surface for casting is suggested to eliminate changes of thickness of the samples during casting and while hardening.

Preparation of Materials

Biochar's natural tendency to maintain humidity level above 40% was one of the most difficult issues in this study. Higher levels of humidity caused prolonged drying time, and possible chemical reactions between biochar and gypsum may have caused inconsistent results in experimental groups.

Additionally, testing moisture content of biochar on days of mixing is recommended for future research to minimize random effects due to different humidity levels of the materials.

Recommendations for Future Research

This research focused only on three basic properties of biochar-gypsum as a starting point. Replicating the study in a manufacturing facility is recommended to accurately compare the thermal conductivity, flexural strength, and density of biochar-gypsum to those of manufactured gypsum board with no additives.

Other potential investigations include other properties of the composite, such as fire resistance, pull resistance, ability to accept finishes, which are tested by ASTM C1396.

Another issue for future empirical research on biochar-gypsum is to study the ability of biochar to maintain constant humidity levels, which has the potential to raise the indoor air quality (IAQ) sustainability rating for the composite interior finish material, and provide healthier environment for occupants. Maintaining constant humidity levels through biochar's inclusion in gypsum board will also reduce the consumption of energy needed for running humidifier during the cold seasons.

Additionally, the ability of biochar-gypsum to sequester carbon dioxide needs to be tested, as this characteristic of the composite has the potential to improve not only the indoor air quality for the inhabitants but have a positive impact on the environment.

Studying the chemical reactions between biochar and gypsum is recommended to better understand the behavior of the composite material and optimize its properties for manufacturing of this new bio-based material.

To close the loop, the effect of biochar-gypsum waste from production and construction should be investigated for its ability to improve fertility of land, and as a vehicle to negate floods due to the ability of biochar to retain moisture. The literature review indicated substantial research on use of biochar alone and gypsum alone as soil amendments. The effect of the biochar-gypsum composite on soils needs to be studied as chemical reactions may alter the properties of the mix.

REFERENCES

Abdi, H., & Williams, L. J. (2010). Tukey's honest significant difference test. In N. Salkind (Ed.). *Encyclopedia of research design*. Thousand Oaks, CA: Sage.

Abu-Lebdeh, T., Fini, E., & Fadiel, A. (2014). Thermal conductivity of rubberized gypsum board. *American Journal of Engineering & Applied Sciences, 7*(1), 12-22.

Allen, E., & Iano, J. (2014). *Fundamentals of building construction: Materials and methods* (6th ed.). Hoboken, NJ: John Wiley & Sons.

Anthony, V. (Ed.). (2010). *Instrumentation*. Center for the Advancement of Process Technology. Upper Saddle River, NJ: Pearson Education.

Arch Media Group LLC. (n.d.). *Archtoolbox, Architect's technical reference*. Retrieved from https://www.archtoolbox.com/materials-systems/thermal-moisture-protection/rvalues.html

ASHRAE Standard 100-2015. (2015). *Energy efficiency in existing buildings*. Retrieved from http://www.techstreet.com/ashrae/searches/8487309

ASTM Committee E-6. (1999). *ASTM E699 - 99 standard criteria for evaluation of agencies involved in testing, quality assurance, and evaluating building components in accordance with test methods promulgated by ASTM Committee E-6*. Retrieved from http://www.astm.org/DATABASE.CART/HISTORICAL/E699-99.htm

ASTM International. (2014a). *Standard specification for woven wire test sieve cloth and test sieves.* (Designation: E11). Retrieved from https://www.astm.org/Standards/E11.htm

ASTM International. (2014b). *Standard terminology relating to gypsum and related building materials and systems.* (Designation C11-14). Retrieved from https://www.astm.org/Standards/C11.htm

ASTM International. (2014c). *Standard specification for gypsum plasters*. (Designation: C28). Retrieved from http://www.astm.org/Standards/C28.htm

ASTM International. (2014d). *Standard test method for steady-state thermal performance of building assemblies by means of a guarded hot box.* (Designation: C236). Retrieved from http://www.astm.org/Standards/C236.htm

ASTM International. (2014e). *Standard test methods for physical testing of gypsum panel products*. (Designation: C473-12) Retrieved from http://www.astm.org/Standards/C473.htm

ASTM International. (2014f). *Standard specification for joint compound and joint tape for finishing gypsum board*. (Designation: C475-14) Retrieved from http://www.astm.org/Standards/C475.htm

ASTM International. (2014g). *Standard specification for gypsum board*. (Designation: C1396). Retrieved from http://www.astm.org/Standards/C1396.htm

Biocore. (2014). *What is lignocellulosic biomass?* Retrieved from http://www.biocore-europe.org/pagee027.html?optim=what-is-lignocellulosic-biomass--

Cohen, J. (1988). *Statistical power analysis*. Hillsdale, NJ: Erlbaum.

ColoradoENERGY. (2013). *R-Value table. Insulation values for selected materials*. Retrieved from http://www.coloradoenergy.org/procorner/stuff/r-values.htm

Davis, J. G., & Whiting, D. (2013). *Choosing a soil amendment.* Retrieved from http://extension.colostate.edu/topic-areas/yard-garden/choosing-a-soil-amendment/

Department of Biostatistics, Vanderbilt University. (2013). *PS: Power and sample size calculation*. Retrieved from http://biostat.mc.vanderbilt.edu/wiki/Main/PowerSampleSize#Downloading_and_Installing_the_PS_Software

Drochytka, R., Zach, J., Korjenic, A., & Hroudove, J. (2013). Improving the energy efficiency in buildings while reducing the waste using autoclaved aerated concrete made from power industry waste, *Energy and Buildings, 58*, 319-323. Retrieved from http://dx.doi.org/10.1016/j.enbuild.2012.10.029

Ellis, P. D. (2006). *What is the ideal level of statistical power?* Retrieved from https://effectsizefaq.com/2010/05/31/what-is-an-ideal-level-of-statistical-power/

The Engineering Toolbox. (n.d.). *Thermal conductivity of some common materials and gases.* Retrieved from http://www.engineeringtoolbox.com/thermal-conductivity-d_429.html

Feldman, D., Banu, D., Hawes, D., & Ghanbari, E. (1991). Obtaining an energy storing building material by direct incorporation of an organic phase change material in gypsum wallboard. *Solar Energy Materials, 22,* 231-242. doi:10.1016/0165-

1633(91)90021-C

Feustel, H., & Stetiu, C. (1997). *Thermal performance of phase change wallboard for residential cooling application*. Retrieved from http://eetd.lbl.gov/newsletter/cbs_nl/nl16/cbs-nl16-phase.html

Folger, P. (2014). *Carbon capture and sequestration: Research, development, and demonstration at the U.S. Department of Energy.* Retrieved from http://www.fas.org/sgp/crs/misc/R42496.pdf

Frohnsdorff, G., & Masters, L. W. (1980). The meaning of durability and durability prediction. In Serada, P.J., & Litvan, G.G. (Eds.), *Durability of Building Materials and Components: Proceedings of the First International Conference* (pp. 17-30). Baltimore, MD: American Society for Testing and Materials

Garcia-Perez, M., Lewis, T., & Kruger, C. E. (2010). *Methods for producing biochar and advanced biofuels in Washington State. Part 1: Literature review of pyrolysis reactors. First project report.* Department of Biological Systems Engineering and the Center for Sustaining Agriculture and Natural Resources. Pullman, WA: Washington State University.

General Services Administration. (2015). *PBS-P100 Facilities standards for the public buildings service.* Retrieved from http://wbdg.org/ccb/GSAMAN/p100_2015.pdf

Georgia-Pacific. (2016). *Manufacturing gypsum board.* Retrieved from http://www.buildgp.com/BPContent.aspx?elementId=10121&repository=bp

GreenTEG. (2016). *Definition of heat flux.* Retrieved from http://www.greenteg.com/heat-flux-sensor/definition-of-heat-flux/

Gutiérrez-González, S., Gadea, J., Rodríguez, A., Junco, C., & Calderón, V. (2011). Lightweight plaster materials with enhanced thermal properties made with polyurethane foam wastes. *Construction and Building Materials 28*, 653–658 Retrieved from http://www.sciencedirect.com/science/article/pii/S0950061811006040

Gypsum Association. (2010). *Gypsum board typical mechanical and physical properties. GA-235-10*. Retrieved from http://www.pabcogypsum.com/sites/default/files/GA-235-10.pdf

Hart, G. H. (2009). *K-Value, U-Value, R-Value, C-Value, Understanding the value in all these values.* Retrieved from http://www.insulation.org/articles/article.cfm?id=IO090302

Hewlett-Packard. (n.d.). *HP3478 Digital multimeter user manual.* Retrieved from http://www.lightwavestore.com/product_datasheet/EIP-METER-010C_pdf1.pdf

Hukseflux Thermal Sensors. (2006). *User manual HFP01 & HFP03 heat flux plate / heat flux sensor.* Retrieved from http://www.hukseflux.com/sites/default/files/product_manual/HFP01_HFP03_manual_v1620.pdf

Jeffrey, C. (2011). *Construction and demolition waste recycling: A literature review, Dalhousie University's office of sustainability.* Retrieved from http://www.dal.ca/content/dam/dalhousie/pdf/sustainability/Final%20C%26D%20literature%20review.pdf

Kibert, C. J. (2013). *Sustainable construction: Green building design and delivery* (3rd ed.). Hoboken, NJ: John Wiley & Sons.

Kochkin, V. (2010). *High-R walls: Ongoing and planned research.* Retrieved from http://www1.eere.energy.gov/buildings/publications/pdfs/building_america/ns/b6_highr_walls.pdf

Kosny, J., Shukla, N., & Fallahi, A. (2013). *Cost analysis of simple phase change material-enhanced building envelopes in southern U.S. climates*. Retrieved from http://www.nrel.gov/docs/fy13osti/55553.pdf

Laerd Statistics. (2013a). *Independent T-test for two samples*. Retrieved from https://statistics.laerd.com/statistical-guides/independent-t-test-statistical-guide.php

Laerd Statistics. (2013b). *One-way ANOVA in SPSS statistics.* Retrieved from https://statistics.laerd.com/spss-tutorials/one-way-anova-using-spss-statistics.php

Laerd Statistics. (2013c). *Testing for normality using SPSS statistics.* Retrieved from https://statistics.laerd.com/spss-tutorials/testing-for-normality-using-spss-statistics.php

Lee, Y., Park, J., Ryu, C., Gang, K. S., Yang, W., Park, Y-K., Jung, J. & Hyun, S. (2013). Comparison of biochar properties from biomass residues produced by slow pyrolysis at 500^0C. *Bioresource Technology*, *148*, 196-201.

Lehmann, J., Gaunt, J., & Rondon, M. (2006). Bio-char sequestration in terrestrial ecosystems - A review. *Mitigation and Adaptation Strategies for Global Change, 11,* 403–427. doi: 10.1007/s11027-005-9006-5

Level, the Authority on Sustainable Building. (2014). *Material use.* Retrieved from http://www.level.org.nz/material-use/embodied-energy/

MatWeb. (2015). *Material property data.* Retrieved from http://www.matweb.com/reference/flexuralstrength.aspx

McCombs, H. (2015). *LEED Green associate exam preparation guide, LEED v4.* Orland Park, IL: American Technical Publisher.

McCrum-Gardner, E. (2010). Sample size and power calculations made simple. *International Journal of Therapy and Rehabilitation, 17*, 01.

Mehta, M., Scarborough, W., & Armpriest, D. (2010). *Building construction: Principles, materials, and systems.* Upper Saddle River, NJ: Pearson Prentice Hall.

Miedema, J., & Flora, G. (2011). *Declaration of sustainability for biochar production. U.S. biochar initiative.* Retrieved from http://www.biochar-international.org/sites/default/files/Biochar_Sustainability_Protocols_March_2011_Draft.pdf

Minitab. (2016). *Minitab's power and sample size tools.* Retrieved from https://www.minitab.com/en-us/Published-Articles/Minitab-s-Power-and-Sample-Size-Tools/

MTS Systems Corporation. (2007). *MTS Insight 5 material testing product information.* Retrieved from http://www.mts.com/cs/groups/public/documents/library/dev_004543.pdf

MTS Systems Corporation. (2016). *MTS 661.20 Force transducer.* Retrieved from https://www.mts.com/cs/groups/public/documents/library/dev_003708.pdf

National Instruments. (2015). *User guide NI USB6008/6009 bus-powered multifunction DAQ USB device.* Retrieved from http://www.ni.com/pdf/manuals/371303n.pdf

National Instruments. (2016). *What can you do with LabVIEW?* Retrieved from http://www.ni.com/labview/why/

National Joint Apprenticeship and Training Committee. (2008). *Fundamentals of instrumentation* (2nd ed.). Clifton Park, NY: Delmar Cengage Learning.

Newsom, J. (2006). *Post Hoc tests*. Retrieved from www.upa.pdx.edu/IOA/newsom/da1/ho_posthoc.doc

Office of Energy Efficiency & Renewable Energy. (2013). *Glossary of energy–related terms.* Retrieved from http://energy.gov/eere/energybasics/articles/glossary-energy-related-terms#H

Office of Energy Efficiency & Renewable Energy. (2014a). *Advanced energy designs.* Retrieved from http://energy.gov/eere/buildings/advanced-energy-design-guides

Office of Energy Efficiency & Renewable Energy. (2014b). *About the Building Technologies Office*. Retrieved from http://energy.gov/eere/buildings/building-technologies-office

Peláez-Samaniego, M. R., Garcia-Perez, M., Cortez, L. B., Rosillo-Calle, F., & Mesa, J. (2008). Improvements of Brazilian carbonization industry as part of the creation of a global biomass economy. *Renewable and Sustainable Energy Reviews, 12*(4), 1063-1086.

Pew Center on Global Climate Change. (2011*). ClimateTech book: Building envelope.* Retrieved from http://www.c2es.org/docUploads/BuildingEnvelope.pdf

RapidTables Online References and Tools. (n.d.). *Watts to BTU per hour conversion.* Retrieved from http://www.rapidtables.com/convert/power/Watt_to_BTU.htm

Reddy, N. (2010). *Biochar bricks for construction*. Retrieved from http://e-biocharbricks.blogspot.com/

Reddy, N. (2013). *Sustainability of biochar systems in developing countries.* Retrieved from http://www.biochar-international.org/Sustainability_Biochar_Systems_DevelopingCountries

Renewable Energy Institute. (2003). *Flue gas desulfurization*. Retrieved from http://fluegasdesulfurization.com/

Sandler, K. (2003). *Analyzing what's recyclable in C&D debris*. Retrieved from https://www.highbeam.com/doc/1P3-475183061.html

Schmidt, H. P. (2012). 55 uses of biochar. *Ithaka Journal, 1,* 286–289. Retrieved from http://www.ithaka-institut.org/en/biochar products

Schossig, P., Henning, H. M., Gswander, S., Haussmann, T. (2005). Micro-encapsulated phase change materials integrated into construction materials, *Solar Energy Materials And Solar Cells, 89,* 297-306.

Schultmann, F., & Sunke, N. (2007). *Closed-loop oriented project management in construction: An approach for sustainable construction management*. Retrieved from http://www.cce.ufl.edu/wp-content/uploads/2012/08/Schultmann.pdf

Setra Systems. (1998). *EL Balance operator's manual.* Retrieved from http://scales.setra.com/pro/manuals/ELManualC.pdf

Simmons, H. L. (2011). *Olin's construction: Principles, materials, and methods* (9th ed.). Hoboken, NJ: John Wiley & Sons.

Skrivanek, S. (2009). *Power of a statistical test*. Retrieved from https://www.moresteam.com/whitepapers/download/power-stat-test.pdf

South Dakota State University. (2016). *METLAB.* Retrieved from http://www.sdstate.edu/mechanical-engineering/metlab

Structall Building Systems. (n.d.). *R Value chart.* Retrieved from http://www.structall.com/pdf/RValue_Chart.pdf

Taylor, J. R. (1997). *An introduction to error analysis*. Sausalito, CA: University Science Books.

Test Products International. (2016). *Dual input K-type thermocouple thermometer with field calibration.* Retrieved from http://testproductsintl.com/wp-content/uploads/2015/04/343-Data-Sheet.pdf

Texas Instruments. (2016). *LM34 Precision Fahrenheit temperature sensors.* Retrieved from http://www.ti.com/lit/ds/symlink/lm34.pdf

US Department of Agriculture. (2014). *What is pyrolysis?* Retrieved from http://ars.usda.gov/Main/docs.htm?docid=19898

US Department of Energy. (2015). *Building energy codes program*. Retrieved from http://www.energycodes.gov/resource-center/glossary/b

US Environmental Protection Agency. (2012). *Waste reduction model (WARM), version 12.* Retrieved from http://www.epa.gov/epawaste/conserve/tools/warm/

USGBC Research Committee. (2008). *A national green building research agenda*. Retrieved from http://www.usgbc.org/Docs/Archive/General/Docs3402.pdf

USGBC. (2016). *US green building council*. Retrieved from http://www.usgbc.org/organizations/us-green-building-council

US Geological Survey. (2014). *Mineral commodity summaries-gypsum.* Retrieved from http://minerals.usgs.gov/minerals/pubs/commodity/gypsum/mcs-2014-gypsu.pdf

XLStat. (2015). *Welch and Brown-Forsythe one-way ANOVA.* Retrieved from https://www.xlstat.com/en/solutions/features/welch-and-brown-forsythe-one-way-anova

APPENDIX A

TERMS

Advanced Energy Design Guides (AEDGs) -- a product of the US Office of Efficiency & Renewable Energy, “accelerate the construction of energy efficient buildings by providing prescriptive solutions to achieve significant energy savings over minimum building energy codes” (Office of Energy Efficiency, 2014a, p.1).

Biochar—“pyrolysis of biomass produces three products: one liquid, bio-oil, one solid, bio-char and one gaseous (syngas)” (US Department of Agriculture, 2014, p.1).

Biomass—“the product of photosynthesis from carbon dioxide and water” (Lee et al., 2013, p. 196).

Building envelope –“is the interface between the interior of the building and the outdoor environment, including the walls, roof, and foundation” (Pew Center on Global Climate Change, 2011, p. 1).

Building Technologies Office – a part of the US Office of Efficiency & Renewable Energy, “leads a network of research and industry partners to continually develop innovative, cost-effective, energy-saving solutions for homes and buildings” (Office of Energy Efficiency, 2014b, p.1).

Calcining-- gypsum is “quarried, crushed, dried, ground to a fine powder, and heated to 350 degrees Fahrenheit (175^0C) in a process known as calcining to drive off about three quarters of its water of hydration” (Allen & Iano, 2014, p. 893).

Carbon sequestration – “is a physical process that involves capturing manmade carbon dioxide (CO_2) at its source and storing it before its release to the atmosphere” (Folger, 2014, p. 1).

Closed-loop – “use of recovery concepts already widely spread in the manufacturing industry, e. g. reuse, refurbishing or recycling” (Schultmannn & Sunke, 2007, p. 2).

Embodied energy—“is the total energy required for the extraction, processing, manufacture and delivery of building materials to the building site” (Level, the Authority on Sustainable Building, 2014, p.1).

Flexural strength of a material is defined as its ability to “resist deformation under load” (MatWeb, 2015, p. 1).

Flexural strength of gypsum panel without surfacing material, is determined by the “average breaking load in pound force (lbf.)” (ASTM International, 2014e, p. 2).

Flue gas desulfurization (FGD)—“ is the technology or process used that removes sulfur oxides and sulfur dioxides (SO_2) from the products of combustion or flue gases at power plants (biomass or coal fueled) that are produced in boilers” (Renewable Energy Institute, 2003, p.1).

Green Building – “is a facility designed using a holistic and collaborative process that addresses a life-cycle resource consumption, environmental impacts and the health of the occupants and local ecosystems” (Kibert, 2013, p. 529).

Gypsum board, also known as wallboard, drywall, gypsum wallboard (GWB) and plasterboard, “is a prefabricated plaster sheet material…sandwiched between special paper faces” (Allen & Iano, 2014, p. 912).

Heat flux – “Heat Flux is the rate of heat energy that passes through a surface. Its units can be expressed as W/m^2” (GreenTEG, 2016, p. 1).

Heat flux sensor – “serves to measure the heat that flows through the object in which it is incorporated” (Hukseflux Thermal Sensors, 2006, p. 5).

Heat transfer –“The flow of heat from one area to another by conduction, convection, and/or radiation” (Office of Energy Efficiency, 2013. p. 1).

High-performance building – “is the terminology used to more specifically define the intended outcome of a green building design and construction process” (Kibert, 2013, p. 529).

LEED, Leadership in Energy and Environmental Design – “is an internationally recognized green building certification system developed by the USGBC and administered by the Green Building Certification Institute” (Kibert, 2013, p. 530).

Life cycle assessment (LCA) – “is an analysis of the environmental impacts and potential impacts associated with a product, process, or service process” (Kibert, 2013, p. 530).

Lignocellulosic materials –“plant biomass that is composed of cellulose, hemicellulose, and lignin” (BioCore, 2014, p. 1).

Pyrolysis –“the heating of an organic material, such as biomass, in the absence of oxygen” (US Department of Agriculture, 2014, p. 1).

R-Value – “indicates the thermal resistance of a material. The R-value of thermal insulation depends on the type of material, its thickness, and its density. The higher the R-value, the greater is the insulating effectiveness. In calculating the R-value of a multilayered installation, the R-Values of the individual layers are added” (Kibert, 2013, p. 532).

Renewable materials – “are materials that have a short renewal cycle and require limited processing to convert to a usable form” (Mehta, Scarborough & Armpriest, 2010, p. 205).

Soil amendment – “is any material added to a soil to improve its physical properties, such as water retention, permeability, water infiltration, drainage, aeration and structure” (Davis & Whiting, 2013, p.1).

Sustainable development – “is development that meets the needs of the present without compromising the ability of future generations to meet their own needs” (Kibert, 2013, p. 533).

Synthetic gypsum, or FGD (flue gas desulfurization) gypsum —“ is the technology or process used that removes sulfur oxides and sulfur dioxides (SO_2) from the products of combustion or flue gases at power plants (biomass or coal fueled) that are produced in boilers” (Renewable Energy Institute, 2003, p.1).

Sulfur dioxide gas – “under certain conditions the drywall may produce hydrogen sulfide gas. Incineration can produce sulfur dioxide gas” (EPA, 2012, p. 2).

Thermal conductivity–“The rate of heat flow, under steady conditions, through unit area, per unit temperature gradient in the direction perpendicular to the area. It is

given in the SI units as Watts per (meter – Kelvin)" (The Engineering Toolbox, n.d., p. 1).

Thermal resistance, R-value, is the reciprocal of thermal conductivity, e.g. R=1/U (Kibert, 2013, p. 534).

U.S. Green Building Council, or USGBC – "is a 501(c) (3) nonprofit organization committed to a prosperous and sustainable future for our nation through cost-efficient and energy-saving green buildings." (USGBC, 2016, p.1).

APPENDIX B

HFP01 CALIBRATION CERTIFICATE-HUKSEFLUX

Hukseflux
Thermal Sensors

Hukseflux Thermal Sensors B.V.
www.hukseflux.com
info@hukseflux.com

Product certificate

Pages: 1
Release date: 22-04-2016

Product code	**HFP01-05**
Product identification	**serial number 12229**
Product type	heat flux plate / heat flux sensor
Measurand	heat flux
Calibration result	
Sensitivity	**S = 61.70 x 10^{-6} V/(W/m^2)**
Calibration uncertainty	**± 1.85 x 10^{-6} V/(W/m^2)**
	the number following the ± symbol is the expanded uncertainty with a coverage factor k = 2, and defines an interval estimated to have a level of confidence of 95 percent
Measurement function	Φ = U/S With Φ heat flux in [W/m^2], U voltage output in [V]
Product specifications	
1: cable length	**5 m**

Table 0.1 *connections*

WIRE	
Black	ground
White	signal [+]
[redacted]	signal [−]

Calibration procedure according to Hukseflux HFPC01.
Traceability of calibration is to SI units.

Please consult the user manual for information on measurement uncertainty during actual use and for product set up, operation and maintenance instructions.

Calibration performed by:
G Spierings

Date:
21-04-2016

Person authorising acceptance and release of product:
G.J. Halve

Date:
22-04-2016

Figure B1. HFP01 Calibration Certificate from Hukseflux Thermal Sensors

APPENDIX C

SAMPLE THICKNESS MEASUREMENTS

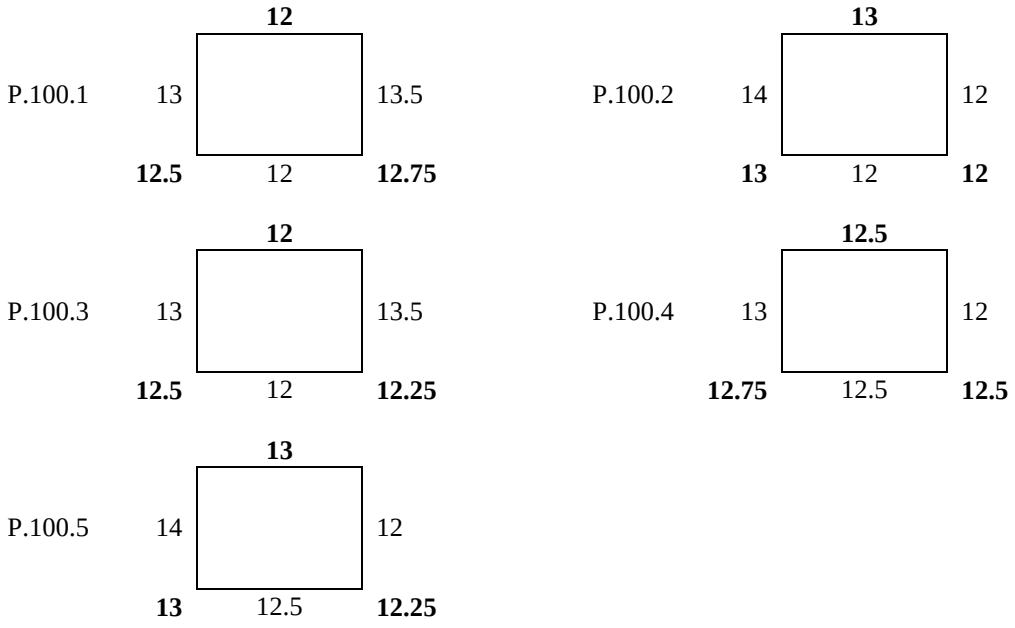

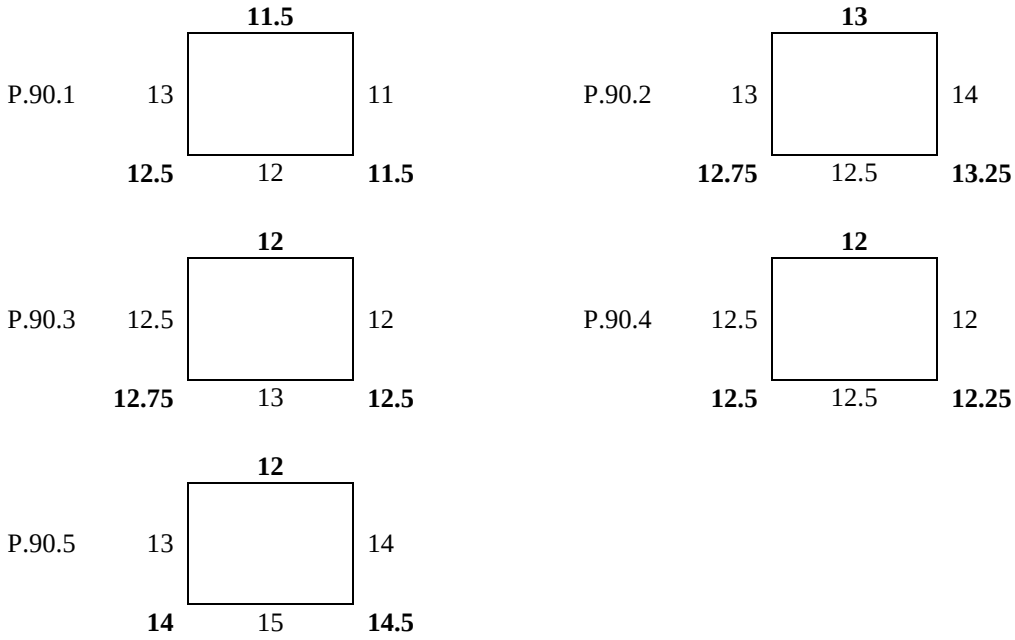

(figure continues)

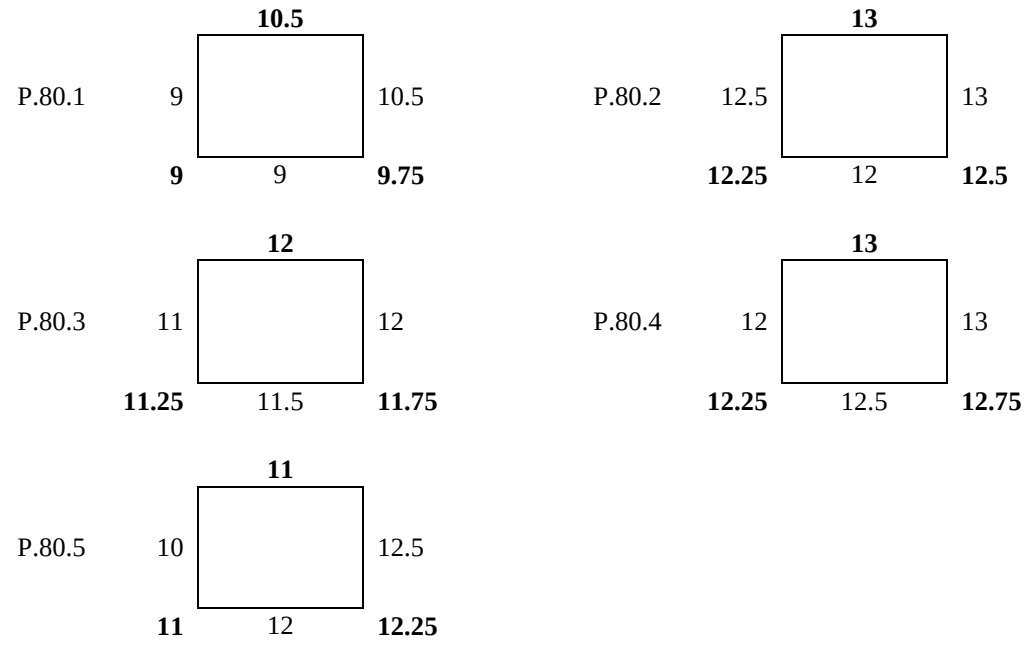

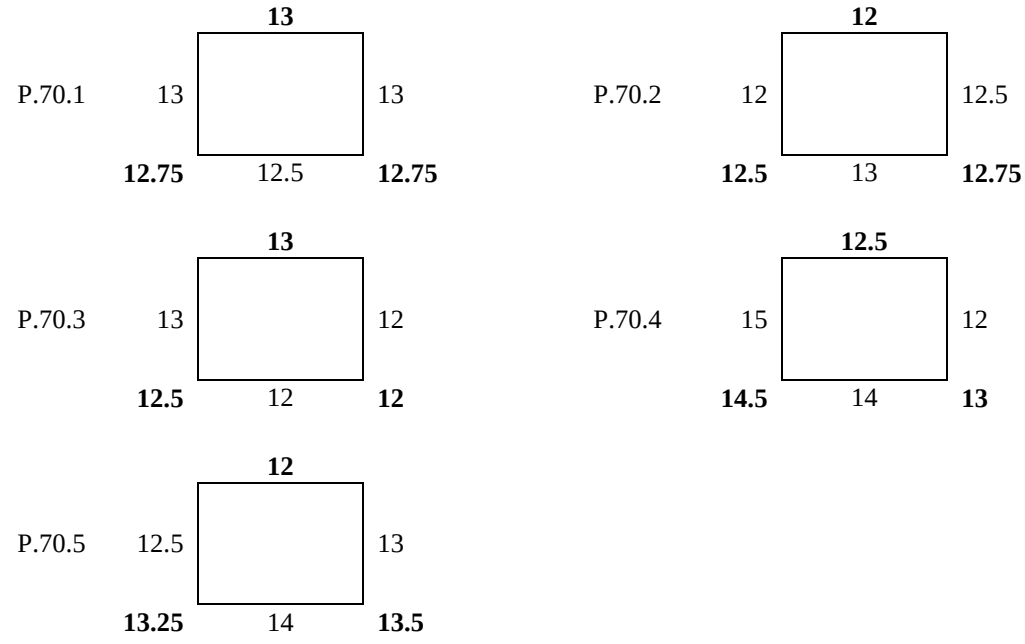

(figure continues)

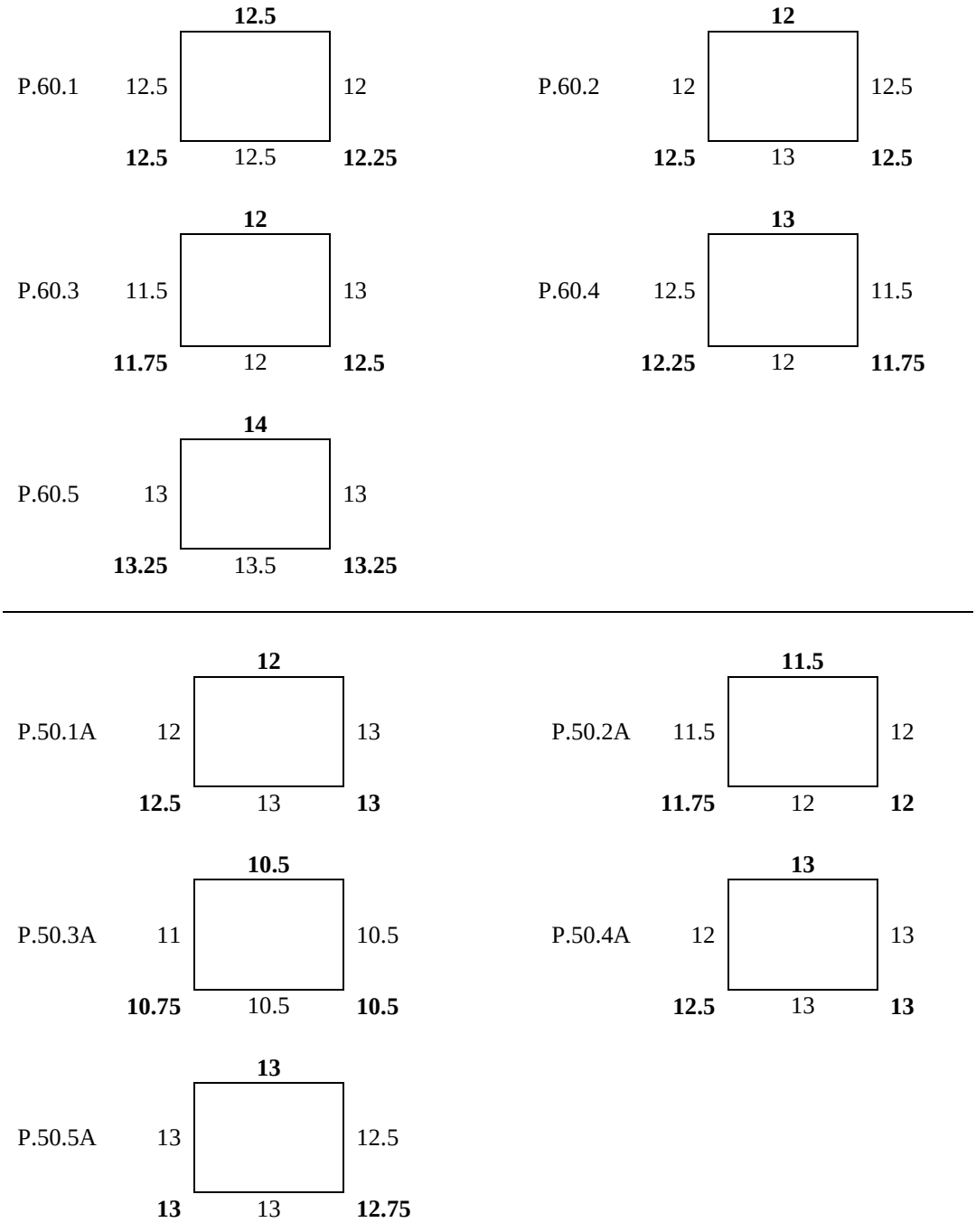

Figure C1. Sample thicknesses (mm). Samples are measured in the middle of each side. Sensor Pairs 1 and 3 are midway between the side measurements. Sensor Pair 2 is the same as the top measurement. Numbers in bold are used for k calculations. See graphical explanation in Chapter 3, Thermal Conductivity Measurement Test Procedure Section

APPENDIX D

DENSITY MEASUREMENTS OF SAMPLES

Table D1

Density Measurements and Calculations for Control and Experimental Samples

				Thickness in middle of edge				Average		
	weight	length	width	Front	Right	Back	Left	thickness	volume	Density
	grams	cm	cm	mm	mm	mm	mm	cm	cm^3	g / cm^3
P.100.1	1474	30.7	30.7	12	13.5	12	13	1.2625	1189.894	1.239
P.100.2	1474	30.6	30.6	12	12	13	14	1.275	1193.859	1.235
P.100.3	1412	30.8	29.9	12.5	12	12	13	1.2375	1139.639	1.239
P.100.4	1460	30.8	29.8	12.5	12.5	12.5	13	1.2625	1158.773	1.260
P.100.5	1423	30.8	30.5	12.5	12	13	12	1.2375	1162.508	1.224
P.90.1	1360	30.7	30.6	12	11	11.5	13	1.1875	1115.561	1.219
P.90.2	1525	30.6	30.5	12.5	14	15	13	1.3625	1271.621	1.199
P.90.3	1258	30.7	29.8	13	12	12	12.5	1.2375	1132.139	1.111
P.90.4	1249	30.8	30.5	12.5	12	12	12.5	1.225	1150.765	1.085
P.90.5	1469	30.5	30.6	15	14	12	13	1.35	1259.955	1.166
P.80.1	947	30.7	30.7	9	10.5	10.5	9	0.975	918.928	1.031
P.80.2	1303	30.7	30.8	12	13	13	12.5	1.2625	1193.770	1.092
P.80.3	1172	30.8	30.5	11.5	12	12	11	1.1625	1092.053	1.073
P.80.4	1186	30.8	30.0	12.5	13	13	12	1.2625	1166.550	1.017
P.80.5	1071	30.9	29.9	12	12.5	11	10	1.1375	1050.948	1.019
P.70.1	1315	30.6	30.7	12.5	13	13	13	1.2875	1150.000	1.143
P.70.2	1182	30.8	29.9	14	13	12.5	12.5	1.3	1197.196	0.987
P.70.3	1213	30.8	29.9	13	13	14	13.5	1.3375	1231.731	0.985
P.70.4	1393	30.7	30.6	15	12	12	15	1.35	1268.217	1.098
P.70.5	1254	30.8	30.5	13	12.5	12.5	12	1.25	1174.250	1.068
P.60.1	1172	30.4	29.8	12.5	12	12.5	12.5	1.2375	1121.076	1.045
P.60.2	1135	30.0	30.4	13	12.5	12	12	1.2375	1128.600	1.006
P.60.3	1114	30.5	30.5	12	13	12	11.5	1.2125	1127.928	0.988
P.60.4	1221	30.7	30.7	12	11.5	13	12.5	1.225	1154.550	1.058
P.60.5	1324	30.7	30.4	13.5	13	14	13	1.3375	1248.262	1.061
P.50.1A	1072	30.7	30.6	13	13	12	12	1.25	1174.275	0.913
P.50.2A	962	30.5	29.8	12	12	11.5	11.5	1.175	1067.958	0.901
P.50.3A	825	30.0	30.4	10.5	10.5	10.5	11	1.0625	969.000	0.851
P.50.4A	1104	30.7	30.5	13	13	13	12	1.275	1193.846	0.925
P.50.5A	1146	30.6	30.6	13	12.5	13	13	1.2875	1205.564	0.951